HHS Public Access

Author manuscript

Magn Reson Imaging Clin N Am. Author manuscript; available in PMC 2022 November 01.

Published in final edited form as:

Magn Reson Imaging Clin N Am. 2021 November ; 29(4): 557–581. doi:10.1016/j.mric.2021.06.007.

Fetal Neuroimaging Updates

Jeffrey N Stout, PhD[##],
Fetal and Neonatal Neuroimaging and Developmental Science Center, Department of Pediatrics, 300 Longwood Ave, Boston, MA, 02115.

M. Alejandra Bedoya, MD[#],
Department of Radiology, Boston Children's Hospital, 300 Longwood Ave, Boston, MA, 02115

P. Ellen Grant, MD MSc[#],
Fetal and Neonatal Neuroimaging and Developmental Science Center, Departments of Radiology and Pediatrics, Boston Children's Hospital, Boston Children's Hospital, 300 Longwood Ave, Boston, MA, 02115

Judy A. Estroff, MD[#]
Section Chief Fetal Neonatal Imaging, Department of Radiology, Maternal Fetal Care Center, Boston Children's Hospital, 300 Longwood Avenue, Boston, MA, 02115

[#] These authors contributed equally to this work.

Keywords

• Fetus; • Magnetic resonance imaging; • Neuroimaging

Introduction

Fetal ultrasound (US) and magnetic resonance imaging (MRI) provide essential information in the evaluation and management of pregnancies and have been shown to improve perinatal outcomes in cases that require antenatal or perinatal surgical and medical intervention.[1] The information provided by fetal imaging is important both to prospective parents and to the many specialists who counsel them, and it allows for more accurate diagnosis and determination of prognosis.

US and MRI are complementary modalities in fetal neuroimaging. US is the first-line imaging modality and thus plays an important role in screening, identification, characterization and follow up of fetal and placental abnormalities. US provides high spatial and temporal resolution, color and spectral Doppler assessment, and has 3D volume rendering capabilities, important in lesion characterization. The American College

[#]JNS is the corresponding author. jeffrey.stout@childrens.harvard.edu.

Disclosures: The authors have no commercial or financial conflicts of interest to declare.

of Radiology (ACR) in conjunction with the American College of Obstetricians and Gynecologists (ACOG) and the American Institute of Ultrasound in Medicine (AIUM) recommend that the US evaluation of the fetal head, face and neck should routinely include images of the lateral cerebral ventricles, choroid plexus, cerebellum, cisterna magna, midline falx, cavum septum pellucidum, and upper lip.[2] A significant advantage of US in the evaluation of the fetal brain is the availability of extensive normative biometric data and the reliable assessment of cranial size in cases of possible microcephaly or macrocephaly.[3] Table 1 summarizes the advantages and disadvantages of fetal US and fetal MRI sequences.

MRI can be used as a complementary modality that provides additional information when US is unable to clearly characterize an abnormality, or when the abnormality is suspected but may be sonographically occult. A fetus with a suspected brain abnormality on screening US, or with a high family risk for brain abnormalities, should undergo fetal MRI as it offers better contrast, higher resolution, and has multiplanar capabilities which increase the accuracy and confidence in the detection of fetal brain abnormalities.[4] This was demonstrated by a multicentre, prospective cohort study of 570 fetuses by Griffiths et al. In this study, MRI had a higher accuracy in the diagnosis of fetal brain abnormalities compared to US (93% versus 68%), provided additional information in 49% of the cases, changed prognostic information in 20% of cases, and led to changes in clinical management in more than 30% of the cases.[5] A recently published meta-analysis that included 27 articles in 1184 fetuses,[6] demonstrated that fetal MRI was concordant with postnatal diagnosis in 80% of the cases, compared to 54% concordance with US. Nevertheless, fetal MRI should be performed and interpreted with same-day or concurrent US, as the two modalities provide different and complementary information, particularly in the assessment of extracranial head/neck and spine abnormalities.

Neuroimaging of the developing brain, face/neck and spine of the fetus is complex, but crucial. Interpreting and reporting fetal MRI requires not only a deep understanding of embryology, normal development and common malformations, but also a clear sense of the MR sequences currently available for clinical use, their limitations and artifacts commonly seen. This manuscript will focus on current state-of-the-art MRI sequences used in fetal neuroimaging, with a specific focus on current clinical applications, complementary contribution compared with US, and future directions to improve image quality.

Fetal MR: Background

Physics background

Fetal MRI uses hardware that has been optimized for other adult and pediatric applications (e.g. brain, heart, body and joint imaging) and this can result in poor image quality which is outside the operator's control. A brief overview of MRI physics is necessary to understand the operator independent effects of image quality. To create an image using an MR scanner, radio frequency (RF) waves are used to excite protons which then resonate at a frequency determined by the magnetic field strength at that location. Gradients, spatially varying magnetic fields, are applied to encode location, which permits imaging. The series of RF and gradient pulses give rise to the common MRI physics phrase "pulse sequence" to describe how a specific image is acquired. The external field is known as B_0 and the fields created

by the RF waves B_1. En masse the resonating protons are detected by receive coils, and the resulting signals processed to create an image.

Basic imaging setup

Though true for all MRI, fetal MRI really pressures the quality optimization trade off between signal-to-noise ratio (SNR), speed of image acquisition, and spatial resolution. The field-of-view (FOV) for fetal imaging must typically be large enough so that all the fetal and maternal tissue can be spatially encoded, which prevents maternal tissue from being inadvertently superimposed onto the fetal tissue, an artifact called “aliasing.” With a large FOV, resolution is often coarser than desired for the fetal brain given that higher resolution requires more imaging time to perform the necessary spatial encoding. Ultimately this imaging time is limited by the duration of fetal quiescence or maternal breath hold, thus fetal imaging most often consists of “single-shot” acquisitions where one slice from a volume is acquired at a time. The volume can be acquired over the course of seconds or minutes, but each slice can effectively “freeze” fetal and maternal motion. However, slices and even volumes can be hopelessly corrupted by unpredictable fetal motion, so it is also important to monitor images for motion artifacts and reacquire them when necessary. Table 2 shows an example protocol from our institution conducted on Siemens 3T scanners.

Field strength

There is a linear relationship between SNR and main field strength, such that 3T SNR gains can be traded for more resolution or faster scanning. Fetal scanning at 3T has been shown to be better at detecting both body and brain abnormalities.[7,8] In addition scanning at 3T has been shown to lower RF energy exposure, known as specific absorption rate (SAR).[8,9] However, image artifacts, particularly with steady-state free precession (SSFP) sequences may be worse in some cases.[10] Our institution conducts fetal brain and body scanning at 3T, with fetal cardiac studies conducted at 1.5T. Other factors beyond B_0 strength are important to image quality as well, such as patient comfort related to bore size and gradient and RF performance. When logistical concerns determine scanner choice, as at our institution, both 1.5T and 3T scanners can produce diagnostic quality images.

Dielectric artifact

Dielectric artifacts can be a major nuisance in fetal imaging (Figure 1). They are low spatial frequency signal intensity changes across images.[11] The brighter and darker regions are caused by the constructive and destructive interference of the RF waves used to create MRI images—also known as B_1 inhomogeneity—that have wavelengths shorter than the object being scanned. Wavelength inversely scales with field strength, so at 1.5T wavelengths are ~52 cm but decrease to ~26 cm at 3T, which is smaller than many pregnant abdomens. The practical effect is that if the fetal brain is in a darker region the lower SNR will adversely affect image interpretation or quantification. Thus although 3T MRI comes with SNR advantages, dielectric effects (B_1 inhomogeneities) are a challenge.

Parallel transmit

Parallel transmit systems can be used to reduce or eliminate dielectric effects (B_1 inhomogeneity), producing images that have more uniform baseline signal intensity.[12] The drawback to this approach is that the total power deposited by the RF waves into the body, as heat, is no longer ultimately limited by the transmitter power, but by the geometric relationship between the transmitters, and the magnitude and phase of outputted RF waves.[13,14] These additional degrees of freedom allow the design of RF pulses that obtain certain design specifications, for example a B_1^+ field with variations <5%, and heating below a safety threshold (<2W/kg local SAR), but the workflow and time to design these pulses in real time is a matter of ongoing research.[15–17] The combination of safety concerns for a vulnerable population, lack of temperature modeling, and ongoing technical development means that each MRI system vendor's recommendations should be carefully followed, and as of the April 2020 International Society of Magnetic Resonance in Medicine Placenta and Fetus Study Group meeting on RF Shimming, no consensus recommendation could be promulgated.

Coils

Multichannel phased-array receive coils offer significant SNR advantages because individual coils are closer to the anatomy of interest and the spatial sensitivity of individual coils permits accelerated image acquisition.[18,19] These advantages mean that fetal scanning should leverage the best receive coils available in terms of maternal comfort and channel count. Our institution uses the Siemens 30-channel flexible body array combined with the 18-channel spine array for our fetal examinations and this permits a modest parallel imaging acceleration factor of R = 2. Though there has been some work developing dedicated fetal receive coils,[20,21] the gains are modest in comparison to the latest flexible body coils that can be purchased from the vendors.

Contrast

In animal models, gadolinium-based contrast agents have been shown to cross the placenta, resulting in recirculation through the amniotic fluid during a prolonged period of time.[1] The effect in the developing fetus is unknown; therefore, Gadolinium-based contrast is not approved for use in pregnancy by the U.S. Food and Drug Administration (FDA) and its use in fetal MRI is not recommended.

Ferumoxytol is an ultrasmall superparamagnetic iron oxide (USPION), that is FDA approved for treating iron deficiency anemia in adults with chronic kidney disease. It has also been used off-label in non-pregnant adults as a blood pool agent due to its long half life and as a marker of inflammation because it is taken up by macrophages. As a result there is interest in the use of ferumoxytol as a means to quantify perfusion and inflammation in the placenta. However, use in pregnant women is not yet FDA approved but primate studies of potential diagnostic utility and toxicity are currently underway.[22,23]

Maternal preparation and positioning

Patient preparation is important for the acquisition of high-quality diagnostic images. Some centers advocate for maternal fasting and prohibition of caffeine intake prior to

the examination in efforts to reduce fetal motion and maternal bowel motion; however, there is no evidence to support these recommendations. In 228 pregnant patients who underwent fetal MRI, Yen et al. did not identify a correlation between fetal motion and food and/or caffeinated beverage intake.[24] However, maternal comfort in the scanner is crucial, as studies can be long and maternal discomfort results in maternal anxiety and movement. Scanning is usually performed with an empty bladder and in a supine position with pillows under the knees. However, this is not always possible in late gestational age due to compression of the inferior vena cava, requiring MRI to be performed in left oblique or lateral decubitus maternal positions.

Gestational age challenges

Technically, MRI can be performed at any gestational age; however, the optimal gestational age to perform a fetal MRI depends on the pathology suspected by US as well as maternal size. At our institution we prefer to scan pregnant patients in the larger bore diameter (70 cm) scanners to ensure patient comfort. We have found that the smaller bore diameter systems (60 cm) are suitable before approximately 33 weeks of gestation, and when maternal BMI is less than approximately 30. It is important to consider that there is also a maternal weight limit for each MR scanner.

It is imperative to understand the normal rapidly evolving appearance of the developing fetal brain on MRI. A thorough understanding of embryology is critical for adequate interpretation of fetal MRI. In general, fetal brain development occurs in a predictable pattern with structural morphological changes in cortical sulcation that reflect functional arealization. In addition, parenchymal signal intensity changes reflect the changes happening at the microstructural level during proliferation, cell migration, neuronal organization and maturation.[3] Figure 2 demonstrates the normal progressive development of cerebral sulcation in the fetal brain at different gestational ages, noting that sulcation progresses rapidly from a smooth appearance at 20 weeks gestational age to a highly folded cortex in late gestation. Brain parenchymal signal evolves in a multilayer fashion representing transient zones of brain development (Figure 3).[25] In early fetal stages, between approximately 10 to 17 weeks, 5 to 6 zones can be identified across the cerebral mantle on histopathology: 1) ventricular zone, 2) subventricular zone, 3) intermediate zone, 4) pre-subplate zone, 5) cortical plate, and 6) marginal zone.[26,27] From about 17 weeks, 7 layers can be distinguished across the cerebral mantle on histopathology: 1) ventricular zone, 2) periventricular fiber rich zone, 3) subventricular zone, 4) intermediate zone, 5) subplate zone, 6) cortical plate, and 7) marginal zone.[26] With modern fetal MRI resolutions ~ 1mm in plane using single-shot fast spin echo (SS-FSE) imaging, the marginal zone cannot be detected and the subventricular zone is often difficult to distinguish. In general, 5 layers may be identified: 1) Ventricular zone (T2 hypointense), 2) periventricular fiber-rich zone (T2 hyperintense), 3) intermediate zone (mildly T2 hypointense), 4) subplate zone (T2 hyperintense), and 5) cortical plate (T2 hypointense).[1] The fetal cerebral mantle thickness is less than 10 mm at 20 weeks of gestation and less than approximately 15 mm by week 26 of gestation; therefore the limited resolution and contrast of fetal brain MRIs may result in the ventricular zone, periventricular riber rich zone and subventricular zone appearing as one.[28] Along the caudate nucleus, the ganglion eminence can be visualized as a T2 hypointense

mass. As the fetus advances through the third trimester, the subplate, ventricular zone and ganglionic eminence decrease in size on MRI and by late third trimester, the remaining zones become indistinguishable leaving only the two regions, white matter and cortex.[3] The primitive lateral ventricles are seen at 13 to 14 weeks of gestation and initially appear large and globular in size (Figure 2). With increasing brain development, the lateral ventricles narrow, achieving adult-like configuration by week 16 of gestation. The atrial width of the lateral ventricles is relatively independent of gestational age and therefore it is used to assess ventriculomegaly (greater than 10 mm in atrial width) throughout gestation.[1,29]

For rare clinical indications, fetuses as young as 13–14 weeks may be imaged, but typically referrals for fetal neurological concerns occur from 18 weeks onward. By this stage, early brain development (hemispheric cleavage, commissuration and neuronal proliferation) has already occurred and therefore, abnormalities of these stages, such as holoprosencephaly (abnormality of hemispheric cleavage) can be seen in early gestation. However, cell migration, neuronal organization and maturation is ongoing throughout fetal life, creating a risk of missing a malformation before it is structurally apparent on fetal MRI; for example, gray matter heterotopia are initially very small and therefore difficult to resolve, band heterotopia may be difficult to detect, and lack of normal gyrification, as in lissencephaly/pachygyria, may be difficult to appreciate on early imaging before primary gyri appear.[3] In contrast, visible changes such as globular cavitated germinal matrix, which may seem less important, portend severe malformations that may not yet be fully apparent on imaging.[3]

Fetal movement challenges

Fetal movement is an inherent challenge to fetal MRI, particularly in early pregnancy and in the presence of polyhydramnios.[30] Due to fetal motion, the acquisition of fetal MRI images becomes a dynamic process where the technician is “chasing the fetus” to acquire the necessary images for diagnosis. Strategies to minimize fetal motion-related artifacts include: using the prior sequences as a scout view to prescribe the new orthogonal plane acquisition, decreasing the number of slices, and utilizing ultra-fast sequences (SS-FSE and SSFP). Motion-related artifacts can also originate from maternal breathing, where the abdominal contents shift with diaphragmatic movement; therefore, acquisitions during breath hold aim to mitigate this motion with the drawback of constraining the duration of imaging.[30]

Motion correction aims to preserve image quality by compensating for fetal motion. The two main categories of techniques are retrospective, where motion is corrected after the acquisition of images, and prospective, where motion is corrected during the acquisition.[31] For fetal MRI, retrospective motion correction algorithms are more mature. These tools enable better visualization and characterization of the posterior fossa,[32] improved performance of diffusion tensor images to enable the reconstruction of structural connectivity in the developing brain,[33] and the creation of normal reference atlases for clinical use. Gholipour et al. used a robust slice-to-volume registration algorithm to reconstruct super-resolution volumetric images for each of 6–23 fetuses at each gestational age week that were combined into a normative spatiotemporal atlas of fetal brain development.[34–37] These atlases are available online as a reference for normal fetal brain development at http://fetalmri.org. Prospective motion correction for fetal imaging is being

developed and relies on the volumetric imaging capability of the scanner itself combined with machine vision technology. An automated method of slice prescription has been recently proposed for fetal brain imaging that eliminates the need for a technician to chase the fetal head during the scan.[38] Algorithms have been developed that permit head pose tracking during EPI volume acquisitions,[39] that when combined with automated image quality assessments,[40] may soon enable fully-automated fetal brain MRI.[41] The ultimate goal of these techniques is to make fetal MRI as easy as routine adult brain imaging, with automated systems obviating the training and experience requirements that limit fetal MRI to specialty referral hospitals. Clearly, higher quality acquired images will improve the quality of existing retrospective motion correction outputs.

Sequences used in fetal MRI

Single-shot fast spin echo (SS-FSE)

Technical background—The most widely used MRI sequences for fetal imaging are variants of single-shot fast spin echo (SS-FSE) imaging because it is somewhat robust to fetal motion. This sequence is known as HASTE, SS-FSE, and single-shot TSE by Siemens, GE, and Phillips, respectively. SS-FSE produces an image with T2-weighted contrast. In each “shot”, a single RF excitation is followed by a series of RF refocusing pulses that permit readout of a single image in <300 ms. This approach effectively “freezes” any slow fetal motion, and movements in between shots do not diminish the quality of each image (Figure 1). This primary advantage comes with several current disadvantages. First, the series of shots that make up the sequential slices of a volume are often incoherent, since maternal or fetal motion affects the spatial relationship of the individual images. In the worst case, the fetal anatomy of interest has moved, such that a diagnosis is missed (Figure 4). Second, T_2 decay and T_1 recovery during the readout RF-pulse train introduces blurring and diminishes contrast. Third, the pulse train used for RF refocusing leads to power deposition in the form of tissue heating. To stay under the mandated limits for power deposition of 2W/kg, a delay between shots is introduced by lengthening the repetition time.

Clinical applications—The SS-FSE sequence is the workhorse of fetal imaging and it is the core sequence for structural assessment of the developing fetal brain. It is typically acquired in the three standard orthogonal anatomical planes angulated to the fetal brain. The T2-weighted contrast can provide a clear distinction of the multilaminar appearance of the developing cerebral mantle and show a clear interface between brain parenchyma and extra-axial spaces and the ventricular system. Many review articles and textbooks have shown the utility of SS-FSE images in the detection of cerebral malformations, infections, injuries and mass lesions. [1,3,29,42,43]

SS-FSE is a dark-blood sequence and therefore the presence of flow voids are used to characterize hypervascular lesions such as vascular tumors (congenital hemangioma, benign hemangioendothelioma or kaposiform hemangioendothelioma) and intracranial or extracranial vascular malformations. Congenital hemangiomas are the most common perinatal vascular tumors (Figure 5),[43] characterized by increased vascular mitotic activity during the proliferative phase, which occurs before birth. In contrast, the proliferative/

growth phase in infantile hemangiomas occurs postnatally. In congenital hemangioma, the involution pattern dictates the sub-type, as rapidly involuting congenital hemangioma (RICH), non-involuting congenital hemangioma (NICH), and partially involuting type (PICH). The most common type of congenital hemangiomas in the head and neck are RICH type and, when large, can result in high-output heart failure. Locally aggressive features, such as intracranial invasion and increase in size in the postnatal period should raise the suspicion for benign vascular or kaposiform hemangiothelioma.[43]

Future directions—Ongoing work aims to address the noted disadvantages with SS-FSE imaging. Post-acquisition software tools have been created to reconstruct coherent, super-resolution volumes from multiple incoherent image stacks.[44–48] These reconstruction techniques iteratively register each slice to an estimated template volume, and then resistmate the template volume (Figure 6). Eventually the two steps converge to a consensus volume reconstruction. These have been shown to improve diagnostic utility of these images (Figure 4),[32,49] but integrating these techniques into the clinical workflow remains challenging mainly due to some necessary manual steps, such as determining the initial template volume and initial region of interest. Automated pipelines are in development that may close the loop between SS-FSE acquisitions and the availability of coherent volumes for radiologist interpretation.[50] There is also ongoing work to improve the SS-FSE acquisition itself both by improving its motion robustness and its contrast and image quality.[38,41,51,52] One approach has designed the optimal RF pulse train for developing desired contrast between fetal tissues while minimizing SAR.[52] These acquisition improvements may reduce scan time and fetal SAR exposure, improve the resulting superresolution reconstructions,[53] and perhaps even more importantly, make fetal scanning using SS-FSE available at institutions without the expertise to chase the moving fetus.

Balanced SSFP (bSSFP)

Technical background—Balanced steady-state free precession refers to a type of gradient echo sequence in which the excited magnetization is maintained in the transverse plane by the use of balanced gradient pulses. This sequence is known as TrueFISP, FIESTA, and balanced FFE by Siemens, GE, and Phillips, respectively. This makes bSSFP sequences the most efficient in terms of SNR per unit time. This SNR can be used to acquire higher resolution images, or shorten the time needed to acquire images. bSSFP images can be acquired quickly enough at low resolution (2.2×2.2 mm in plane with 30 mm thick sections permits a temporal resolution of ~300 ms[54]) to create movies of fetal motion. The primary disadvantage of bSSFP images is poor tissue contrast since contrast is approximately T2/T1. This contrast can, nevertheless, be useful if the main objective is to evaluate fetal brain surface topology or to distinguish fetal body anatomy from the surrounding amniotic fluid, when observing fetal motion. bSSFP acquisitions also suffer from banding artifacts that are caused by intravoxel dephasing due to magnetic field inhomogeneities (Figure 1). This is less a problem with modern scanners as they have improved field uniformity, but occasionally this impacts image quality.

Clinical applications—bSSFP is a bright-blood sequence used in conjunction with SS-FSE to evaluate the structural assessment of the developing fetal brain, in particular detection of gyral topology and subtle heterotopias. It is also acquired in the 3 standard anatomical planes aligned to the fetal brain. Fetal motion, in particular fetal swallowing, is one of most common clinical applications of bSSFP sequences acquired as cine clips. Dynamic assessment of fetal swallowing can be evaluated after 12 weeks of gestation[1], providing important information in fetuses with head/neck masses, micrognathia, or in cases of possible tracheoesophageal fistula. Figure 7 demonstrates a case of airway narrowing and swallowing impairment in a fetus with 34 weeks of gestation due to mass effect from a cervical teratoma. Facial/cervical teratomas are usually histologically mature and benign; however, they can result in perinatal death due to airway compromise at birth.[43] Most teratomas demonstrate a mixed cystic and solid appearance with benign teratomas being predominantly cystic, whereas malignant teratomas are usually predominantly solid. Intratumoral hemorrhage and necrosis seen on GRE T2* sequences (see below) suggest an aggressive histology.[43] Fetal MRI plays an important role in delivery planning to include airway team availability during C-section or the ex-utero intrapartum treatment (EXIT) procedure.

bSSFP sequence is not only vital in the evaluation of the head and neck structures, it is also useful in the evaluation of open spinal dysraphism identifying the neural placode and delineating the defect level due to its higher spatial resolution and high contrast between bone and soft tissue/fluid. Spinal dysraphism emcompases a wide spectrum of neural tube defects including both open and closed defects based on the absence (open) or presence (closed) of overlying skin coverage.[55] The presence of skin coverage can be challenging to identify prenatally, but from a fetal surgery perspective, distinguishing an open neural tube defect is crucial, as only an open defect meets criteria for prenatal surgical repair.[56] Taking this into account, prenatal imaging by the combination of fetal US and MRI plays a crucial role in the evaluation of spinal dysraphism (Figure 8). Based on the National Institutes of Health funded Management of Myelomeningocele Study (a.k.a. MOMS trial),[56] some imaging criteria exclude fetuses from prenatal repair of open spinal dysraphism. These exclusion criteria include: maternal conditions (cervix less than 2 cm in length, multiple gestation, placenta previa and maternal Mullerian formation abnormality); fetal brain variables (intracranial abnormality not explained by open spinal dysraphism and absent hindbrain herniation); fetal spine characteristics (kyphosis of more than 30°, upper level of defect higher than T1 and inferior level of defect lower than S1); and other factors (additional fetal anomaly not explained by open spinal dysraphism). The identification of the level of the spinal defect requires the careful complementary assessment by both US and MRI. US provides detail of bony structures[57] and 3D rendering can increase interpretation confidence in the level of the spinal defect. In 61 fetuses with myelomeningocele, Aaronson et al. demonstrated that MRI and US are equally accurate for the assignment of spinal defect level; however, in 20% of cases, both modalities misdiagnosed the spinal level by two or more segments.[58] Using bSSFP sequence, the level of spinal defect can be identified by detecting the L5-S1 level (most caudal hyperintense disc space) and the L5 vertebral body (most caudal horizontal vertebral body).[55]

Future directions—bSSFP sequences rely on the maintenance of a steady-state magnetization to produce high SNR images. One exciting extension of the bSSFP concept is to shift the imaging plane in one direction at a sufficiently slow rate that a front of steady state magnetization is built up that can be swept over the imaging object. This approach has been termed SWEEP, and it generates many overlapping slices with high SNR.[59] When combined with slice to volume registration methods to correct for maternal breathing, a motion corrected coherent volume can be produced (Figure 6).[60] This technique has produced impressive magnetic resonance angiograms of the uterus.[60]

Gradient echo echo planar imaging (GRE-EPI)

Technical background—Echo planar imaging (EPI) permits single slice readouts in less than 100 ms, therefore EPI is very similar to SS-FSE imaging in its motion robustness. T_2* weighted imaging volumes can be obtained in approximately 6 seconds using GRE-EPI. This sequence is so universal it does not have branded names. GRE-EPI permits the acquisition of multiple volumes with repetition times of approximately 3 seconds, that when reviewed in sequence (as a cine) can be used to evaluate fetal motion. The primary disadvantages of GRE-EPI are four classes of imaging artifacts (Figure 1).[61] Ghosting that appears as copies of the observed object overlaid at some interval over the main image. Often called “N/2” or “nyquist” ghosting, it results from slight timing discrepancies in the pulse sequence that arise when gradient hardware is pushed to its maximum specifications to enable the fast switching required by EPI readouts. Geometric distortion transforms normal anatomical structures into abnormal shapes, and is caused by inhomogeneities in B_0 that lead to phase accrual over the long single shot readout. Localized susceptibility artifacts that appear as signal dropouts are caused by rapid intravoxel signal dephasing. This artefact, as discussed below, can be leveraged by comparing short and long TE acquisitions to confirm the presence of blood products or mineralization causing signal dephasing. Chemical shift artifacts can result in areas with high fat content being displaced relative to areas of high water content.

Clinical applications—The magnetic susceptibility artifact related to this sequence is used as an advantage in the identification of calcifications or intracranial hemorrhage. Ventriculomegaly is one of the most common indications for fetal MRI referral, with a wide range of prognostic outcomes ranging from no clinical implications to significant long-term neurodevelopmental sequelae.[29] The etiology of ventriculomegaly is complex and variable with some mechanisms overlapping; however it can be broadly divided into obstructive (subdivided in non-communicating in cases of intrinsic or extrinsic defects of CSF circulation; and communicating in cases of decreased CSF resorption) and non-obstructive, which may be a result of CSF overproduction in choroid plexus lesions, or malformations of brain development with ex-vacuo dilation of the ventricles.[29] Aqueductal stenosis is the classic example of noncommunicating obstructive ventriculomegaly, which could be sporadic, related to genetic or syndromic associations (such as, *L1CAM* mutations), and can be associated with additional brain malformations (such as rhombencephalic or corpus callosal agenesis) or secondary to prior hemorrhage or infection that results in webs or gliotic tissue within the cerebral aqueduct. As seen in Figure 9, EPI T2* sequences play

a vital role in the identification of intraventricular bleeding as one of the causes of non-communicating obstructive ventriculomegaly.

As shown in Figure 10, GRE-EPI cine clips acquired over a few minutes are a relatively new and promising tool in the assessment of subjective fetal motion. GRE-EPI provides an exquisite assessment of the bones and cartilage, with high signal of the cartilaginous epiphyses and low signal of the cortical diaphyseal bone. In fetuses with spinal dysraphism, lower extremity movement can yield important information about the functional defect level, important for parental counseling. Each spinal level can be assessed by the presence or absence of hip flexion (L1), hip adduction (L2), knee extension (L3), knee flexion (L4), ankle dorsiflexion (L5) and ankle plantarflexion (S1).[55] In addition, appendicular movement and fetal breathing motion are indirect markers of fetal wellbeing, included in the fetal biophysical profile [62].

Future directions—EPI and related artifacts have been a topic of research for over 40 years,[63] and so there has been gradual improvement to the MRI hardware that enables artifact minimized EPI on modern scanners. Reduction of EPI scan time has seen improvement by using half-Fourier, parallel imaging and compressed sensing methods.[64–67] Recently, imaging has been greatly accelerated through the advent of simultaneous multi-slice imaging, and new sequences that eliminate distortion and blurring.[68,69] Multi-echo SMS EPI (Table 2) is used at our site for simultaneous fetal motion monitoring, and placental T_2* mapping.[70,71]

Two exciting research applications of fetal EPI data concern fetal motion and fetal brain functional MRI. Tools are now available that permit quantitative fetal motion evaluation using machine learning to identify fetal anatomical key points.[71,72] These motion trajectories may be directly relevant to clinical evaluations of fetal disease, and once calculated during the acquisition may serve as a type of navigator for prospective motion correction of fetal MRI acquisitions.[41] GRE-EPI could also permit fetal brain fMRI, with already promising current results robustly identifying the developing major brain networks.[73,74]

T1-weighted 3D GRE

Technical background—T1-weighted imaging is a workhorse of mature brain imaging, but T1 contrast is difficult to achieve for fetal brain imaging. This difficulty arises from the long duration necessary to create T1 contrast by inversion methods, because waiting for about a second after an inversion pulse to commence image readout makes the sequence prone to fetal motion artifacts. Another approach to T1 contrast is to use a GRE sequence with appropriately selected TR, TE and flip angle to achieve the desired contrast. One drawback of this approach is that typically the required flip angle is not near the Ernst Angle (where maximum SNR can be had for a certain ratio of TR/T1) so T1 contrast comes at the cost of SNR. To claw back some SNR a 3D acquisition is used, and multiple acceleration schemes are employed to minimize the time for fetal motion to cause artifacts. This sequence is known as VIBE, LAVA, and THRIVE by Siemens, GE, and Phillips, respectively.

Clinical applications—T1-weighted images add value in the identification of fetal organs with intrinsic high signal on T1, such as thyroid, pituitary gland and liver (Figure 11); and materials that result in T1 shortening, such as meconium, hemorrhage, fat and calcifications. In addition, T1-weighted images can be used to assess the myelination process, which begins in fetal life and continues in the postnatal period. Lipid content of the myelin demonstrates T1 shortening (high signal in T1-weighted images) in the tegmentum of the pons starting approximately at 23 weeks of gestation and in the posterior limb of the internal capsule at 31 weeks of gestation (Figure 11).[1]

Tissues that demonstrate high signal on T1-weighted images are very limited in the head and neck; therefore, the presence of high signal in this sequence aids in the characterization of some lesions. For example, as shown in Figure 12, fetal goiter is a rare condition with imaging findings that are characteristic. It appears a solid, homogeneous, usually bilobed midline mass around the trachea with increased vascularity on color Doppler interrogation and high-signal on T1-weighted images.[43] Fetal goiter can be the result of maternal thyroid disorders, such as thyroid dysfunction, medication effect, intake of iodine supplements or endemic iodine deficiency; or it could be secondary to a primary fetal thyroid disorder, such as congenital hypothyroidism in the setting of thyroid dysmorphogenesis or due to an error in hormone synthesis or fetal hyperthyroidism.[75] Fetal goiter usually has a benign course; however, it can result in mass effect on the upper airway and esophagus, increasing the risk of polyhydramnios, preterm delivery, hydrops, dystocia and fetal death.[75] Management of fetal goiter depends on its etiology. Adequate management of maternal thyroid disorders can result in resolution of fetal goiter. Profound fetal hypothyroidism, diagnosed via cordocentesis, can be treated with intra amniotic infusion of levothyroxine to decrease the risk of fetal high-output heart failure and fetal hydrops.[76] Because of the potential risk of airway compromise, delivery planning should include airway team availability during C-section or the ex-utero intrapartum treatment (EXIT) procedure.

An additional important clinical application of the T1-weighted sequence is in the identification of thrombosed intracranial vascular malformations. Fetal vein of Galen aneurysmal malformation is a rare congenital malformation that forms between the 6th and 11th weeks of gestation.[77] The median prosencephalic vein, a precursor of the vein of Galen, fails to regress and becomes aneurysmally dilated as a result of cerebral arteriovenous fistulas; therefore, some advocate for the term “median prosencephalic arteriovenous fistulas”. As seen on Figure 13, US and MRI complement each other in the assessment of the vein of Galen aneurysmal malformation. On US, the malformation appears as an anechoic structure in the midline posterior aspect of the third ventricle with increased turbulent arterial and venous flow on Doppler examination. US plays an important role in the identification of flow within the dilated malformation and in the characterization of arterial or venous waveforms in the adjacent vessels. MRI is used to evaluate the relationship with the adjacent brain parenchyma and identification of potential complications, such as cerebral ischemic areas.[77] Complete or partial thrombosis of the dilated vein can be identified on T1-weighted images as an intraluminal high-signal focus. High-flow cerebral shunting can result in increased cardiac preload and high-flow congestive heart failure; which should be evaluated with fetal echocardiography.

Future directions—The challenge with 3D acquisitions for the fetal brain is unpredictable motion. GRE acquisitions that are robust to motion or have integrated motion correction are active areas of research. Non-Cartesian, radial sampling schemes can dramatically improve image quality even in the presence of some motion.[78] There have been Initial implementations of these approaches for fetal brain imaging, but work is needed to improve contrast and specificity of fetal brain tracking.[79] Another approach to compensate for fetal motion is to think about fetal motion as a parameter of interest that can be estimated during the process of image reconstruction. Iterative reconstructions that jointly estimate motion parameters and images have been proposed, though have yet to be applied to fetal imaging.[80,81] Effective fetal motion correction could even permit actual T1-weighted imaging via inversion recovery methods, which would unlock for in-utero use the full set of volumetric morphometry tools that rely on T1 contrast.

Diffusion weighted imaging (DWI) and diffusion tensor imaging (DTI)

Technical background—Diffusion weighted MRI provides information about the directions and magnitude of water diffusion on a voxel-wise basis. It interrogates the subvoxel environment by using magnetic gradients to encode the magnitude and direction of spin movement in the signal intensity of the image. The amount of diffusion weighting is called the “b value” and depends on gradient strength and timing. Diffusion weighted imaging can be read on its own, but parameter maps that summarize the diffusion of water in each voxel, such as the apparent diffusion coefficient (ADC), are important clinical tools. ADC maps require at least four images, three with orthogonal diffusion directions (different b values), and one without any diffusion weighting (b0 image). Fetal motion proves especially challenging to parameter estimation when the component acquisitions are separated in time. Nevertheless DWI and ADC maps are essential to determine fetal brain health in some cases, as despite the typically poor quality of the maps, major shifts in ADC can be detected.

Clinical applications—As with postnatal brain imaging, DWI plays a vital role in the detection and timing of prenatal stroke and hypoxic-ischemic injury. A particular group of fetuses that directly benefits from a complementary assessment of fetal brain MRI and US are fetuses with twin-to-twin transfusion syndrome (TTTS), status post laser ablation therapy. TTTS occurs in approximately 10% of monochorionic twin pregnancies and it is usually identified in the second trimester of pregnancy.[82] Fetoscopic laser-selective coagulation of placental anastomoses (FLSC) is a well-established first line of treatment in severe TTTS. Intracranial complications of FLSC include intraventricular hemorrhage, cystic and non-cystic periventricular leukomalacia, ventriculomegaly and brain parenchymal ischemia.[82] As with the postnatal brain MRI evaluation, DWI sequence plays an important role in identifying cytotoxic edema/parenchymal ischemia, which appears as a decreased diffusion (high signal on high b-value images and low signal on ADC maps) that could be occult on US. US is vital in the identification of postoperative twin anemia polycythaemia sequence (TAPS), which could develop after incomplete laser ablation treatment and increases the risk of prenatal fetal brain injury[82]. TAPS is defined as a peak systolic velocity (PSV) in the middle cerebral artery higher than 1.5 times the Multiple of the Median (MoM) of one twin, representing the fetus with anemia, and of less than 0.8 MoM in the other twin,

representing the fetus with polycythemia [82]. In a group of 1023 cases of TTTS managed with FLSC Stirnemann et al.[82] identified that the overall survival rate of at least 1 twin was 81%, with both twins surviving only in 51%. As shown in Figure 14, DWI sequences are helpful to confirm global decreased brain parenchymal diffusion in cases of fetal demise, which is confirmed with absent cardiac activity on US.

Future directions—Ideally diffusion MRI could be used to learn about the in utero development of structural brain connectivity. To understand structural connectivity, more information about the local tissue microstructure is needed, and this can be obtained with yet more diffusion weighted images. Diffusion tensor imaging (DTI) uses baseline and at least 6 diffusion directions to estimate the diffusion tensor at each voxel permitting structural connectivity mapping. Fetal motion is a profound challenge when trying to perform tractography analysis. Nevertheless, techniques have been developed that permit robust motion correction and tractographic reconstruction of fetal DTI as potential modality to reveal fetal microstructural development and neuro-connectivity (Figure 15).[33] The correspondence of fetal motion detected with the aforementioned techniques and structural brain connectivity is an exciting future direction.

Quantitative physiological imaging, blood flow and oxygenation

Technical background—Beyond structural imaging, MRI can also be used to estimate parameters related to organ perfusion and oxygen consumption. These quantitative methods include the ability to directly measure the velocity of flowing blood using phase contrast MRI (PCMRI), to measure perfusion by magnetically labeling blood to produce an endogenous tracer in a technique called arterial spin labeling (ASL), and to estimate blood oxygen saturation via relaxometry or susceptibility mapping. It is extremely difficult to apply these techniques developed for the adult brain to the fetal brain since it is much smaller, surrounded by maternal tissue that limits imaging resolution, and is free to move. Access to the fetal heartbeat signal which is often used in post-natal MRI exams to gate flow acquisitions is also more difficult. Thus, successful efforts to measure fetal cerebral hemodynamics are extremely impressive given the challenges they face.

PCMRI has been used to explore typical fetal hemodynamics using a retrospective approach to fetal cardiac gating called metric optimized gating (MOG), and by direct US monitoring of the fetal heartbeat using an MRI compatible device.[83,84] MOG has been used to collect data showing how brain sparing physiology, that is the preferential perfusion the brain when flow or oxygenation is limited, is associated with fetal growth restriction.[85]

Motion has largely prevented the application of ASL to the fetal brain given the need for numerous acquisitions to gain sufficient SNR in the small fetal brain with lower cerebral blood flow that neonates.[86] However, there have been numerous attempts to use ASL to better understand placental perfusion.[87–89]

A combination of MOG and estimates of blood oxygenation derived from T2-mapping showed that fetal brain volume was related to ascending aorta oxygen saturation and fetal brain oxygen delivery in cases of CHD.[90] The measurements of fetal cerebral blood flow were based on the superior vena cava (SVC) assuming that this vessel mostly drains the fetal

brain. The fetal brain oxygen extraction fraction was based on the ascending aorta and SVC. Smaller vessels that would better represent brain perfusion alone are beyond the reach of current techniques. The larger umbilical vessels have been targeted using a similar approach to measure the oxygen delivery from the placenta to the fetus.[91] A review of the methods to monitor placental oxygenation and planning for future work in this subfield has been recently published.[92]

Future directions—Once quantitative physiological imaging is sufficiently robust for routine application in utero, there are some immediate high impact applications. Fetal surgical interventions have been developed for a variety of congenital heart defects,[93] and are actively being developed for vein of Galen malformations.[94] As new fetal interventions are proposed these techniques could help with risk stratification and monitoring of therapeutic effect.

Conclusion

Progress in fetal neuroimaging has been challenging, but the promise of improved diagnosis, potential therapeutic benefits of appropriate fetal interventions, and improvements in our understanding of human brain development continue to drive the field forward. MRI's advantages as a non-invasive volumetric imaging modality with good soft tissue contrast make it a strong complement to US screening and diagnosis. However, fetal motion still severely limits the MRI sequences that can be acquired to those that are quick enough to freeze motion. Although there has been very good progress in super-resolution volume reconstructions of the fetal brain after fast single shot image acquisition, FDA approval and timely integration into the clinical workflow is still in progress. However, the field is undergoing rapid advancement, and both prospective and retrospective motion correction strategies promise to make other MRI sequences successful for fetal neuroimaging, improve the performance of existing sequences, and open new horizons to understanding in utero brain development.

Abbreviations:

bSSFP	Balanced steady-state free precession
DWI	Diffusion weighted imaging
DTI	Diffusion tensor imaging
EPI	Echoplanar imaging
FOV	Field of view
GRE	Gradient echo
SAR	specific absorption rate
SNR	Signal to noise ratio
SS-FSE	Single-shot fast spin echo

References

1. Coblentz AC, Teixeira SR, Mirsky DM, Johnson AM, Feygin T, Victoria T. How to read a fetal magnetic resonance image 101. Pediatr Radiol. 2020;50(13):1810–1829. [PubMed: 33252751]
2. AIUM-ACR-ACOG-SMFM-SRU Practice Parameter for the Performance of Standard Diagnostic Obstetric Ultrasound Examinations. J Ultrasound Med. 2018;37(11):E13–E24. [PubMed: 30308091]
3. Choi JJ, Yang E, Soul JS, Jaimes C. Fetal magnetic resonance imaging: supratentorial brain malformations. Pediatr Radiol. 2020;50(13):1934–1947. [PubMed: 33252760]
4. Committee on Practice Parameters – Pediatric Radiology of the ACR Commission on Pediatric Radiology in collaboration with the SPR. ACR–SPR Practice Parameter For The Safe And Optimal Performance Of Fetal Magnetic Resonance Imaging (MRI). The American College of Radiology. Published 2020. Accessed April 6, 2021. https://www.acr.org/-/media/ACR/Files/Practice-Parameters/mr-fetal.pdf
5. Griffiths PD, Bradburn M, Campbell MJ, et al. Use of MRI in the diagnosis of fetal brain abnormalities in utero (MERIDIAN): a multicentre, prospective cohort study. Lancet. 2017;389(10068):538–546. [PubMed: 27988140]
6. van Doorn M, Oude Rengerink K, Newsum EA, Reneman L, Majoie CB, Pajkrt E. Added value of fetal MRI in fetuses with suspected brain abnormalities on neurosonography: a systematic review and meta-analysis. J Matern Fetal Neonatal Med. 2016;29(18):2949–2961. [PubMed: 26592136]
7. Victoria T, Johnson AM, Edgar JC, Zarnow DM, Vossough A, Jaramillo D. Comparison Between 1.5-T and 3-T MRI for Fetal Imaging: Is There an Advantage to Imaging With a Higher Field Strength? AJR Am J Roentgenol. 2016;206(1):195–201. [PubMed: 26700352]
8. Krishnamurthy U, Neelavalli J, Mody S, et al. MR imaging of the fetal brain at 1.5T and 3.0T field strengths: comparing specific absorption rate (SAR) and image quality. J Perinat Med. 2015;43(2):209–220. [PubMed: 25324440]
9. Abaci Turk E, Yetisir F, Adalsteinsson E, et al. Individual variation in simulated fetal SAR assessed in multiple body models. Magn Reson Med. 2020;83(4):1418–1428. [PubMed: 31626373]
10. Weisstanner C, Gruber GM, Brugger PC, et al. Fetal MRI at 3T—ready for routine use? BJR Suppl. 2017;90(1069):20160362.
11. Collins CM, Liu W, Schreiber W, Yang QX, Smith MB. Central brightening due to constructive interference with, without, and despite dielectric resonance. J Magn Reson Imaging. 2005;21(2):192–196. [PubMed: 15666397]
12. Webb AG, Collins CM. Parallel transmit and receive technology in high-field magnetic resonance neuroimaging. International Journal of Imaging Systems and Technology. 2010;20(1):2–13. doi:10.1002/ima.20219
13. Wald LL, Adalsteinsson E. Parallel transmit technology for high field MRI. Magnetom Flash. 2009;40(1):2009.
14. Wald LL, Adalsteinsson E. Specific absorption rate (SAR) in parallel transmission (pTx). MAGNETOM Flash. Published online 2010:65–73.
15. Yetisir F, Turk EA, Guerin B, Others. Potential of parallel transmission for fetal imaging in reducing SAR and mitigating Flip angle inhomogeneities: a simulation study at 3T. In: Annual Meeting of the International Society for Magnetic Resonance in Medicine. ; 2017.
16. Martin A, Schiavi E, Eryaman Y, et al. Parallel transmission pulse design with explicit control for the specific absorption rate in the presence of radiofrequency errors. Magn Reson Med. Published online July 3, 2015. doi:10.1002/mrm.25820
17. Murbach M, Neufeld E, Samaras T, et al. Pregnant women models analyzed for RF exposure and temperature increase in 3T RF shimmed birdcages. Magn Reson Med. 2017;77(5):2048–2056. [PubMed: 27174499]
18. Blaimer M, Breuer F, Mueller M, Heidemann RM, Griswold MA, Jakob PM. SMASH, SENSE, PILS, GRAPPA: how to choose the optimal method. Top Magn Reson Imaging. 2004;15(4):223–236. [PubMed: 15548953]
19. Gruber B, Froeling M, Leiner T, Klomp DWJ. RF coils: A practical guide for nonphysicists. J Magn Reson Imaging. Published online June 13, 2018. doi:10.1002/jmri.26187

20. Chen Q, Xie G, Luo C, et al. A Dedicated 36-Channel Receive Array for Fetal MRI at 3T. IEEE Trans Med Imaging. 2018;37(10):2290–2297. [PubMed: 29994303]
21. Spatz M, Garcia-Polo P, Keil B, Ha C, Wald LL. A 64 channel 3T array coil for highly accelerated fetal imaging at 22 weeks of pregnancy. In: Proc. Intl. Soc. Mag. Reson Vol 25. ; 2017:1220.
22. Nguyen SM, Wiepz GJ, Schotzko M, et al. Impact of Ferumoxytol Magnetic Resonance Imaging on the Rhesus Macaque Maternal-Fetal Interface. doi:10.1101/699835
23. Macdonald JA, Corrado PA, Nguyen SM, et al. Uteroplacental and Fetal 4D Flow MRI in the Pregnant Rhesus Macaque. J Magn Reson Imaging. 2019;49(2):534–545. [PubMed: 30102431]
24. Yen CJ, Mehollin-Ray AR, Bernardo F, Zhang W, Cassady CI. Correlation between maternal meal and fetal motion during fetal MRI. Pediatr Radiol. 2019;49(1):46–50. [PubMed: 30259070]
25. Counsell SJ, Arichi T, Arulkumaran S, Rutherford MA. Fetal and neonatal neuroimaging. Handb Clin Neurol. 2019;162:67–103. [PubMed: 31324329]
26. Kostovic I, Vasung L. Insights from in vitro fetal magnetic resonance imaging of cerebral development. Semin Perinatol. 2009;33(4):220–233. [PubMed: 19631083]
27. Kostovic I, Rakic P. Developmental history of the transient subplate zone in the visual and somatosensory cortex of the macaque monkey and human brain. J Comp Neurol. 1990;297(3):441–470. [PubMed: 2398142]
28. Vasung L, Abaci Turk E, Ferradal SL, et al. Exploring early human brain development with structural and physiological neuroimaging. Neuroimage. 2019;187(vember 2017):226–254. [PubMed: 30041061]
29. Mirsky DM, Stence NV, Powers AM, Dingman AL, Neuberger I. Imaging of fetal ventriculomegaly. Pediatr Radiol. 2020;50(13):1948–1958. [PubMed: 33252761]
30. Machado-Rivas F, Jaimes C, Kirsch JE, Gee MS. Image-quality optimization and artifact reduction in fetal magnetic resonance imaging. Pediatr Radiol. 2020;50(13):1830–1838. [PubMed: 33252752]
31. Maclaren J, Herbst M, Speck O, Zaitsev M. Prospective motion correction in brain imaging: a review. Magn Reson Med. 2013;69(3):621–636. [PubMed: 22570274]
32. Pier DB, Gholipour A, Afacan O, et al. 3D Super-Resolution Motion-Corrected MRI: Validation of Fetal Posterior Fossa Measurements. Journal of Neuroimaging. 2016;26(5):539–544. doi:10.1111/jon.12342 [PubMed: 26990618]
33. Marami B, Mohseni Salehi SS, Afacan O, et al. Temporal slice registration and robust diffusion-tensor reconstruction for improved fetal brain structural connectivity analysis. Neuroimage. 2017;156:475–488. [PubMed: 28433624]
34. Gholipour A, Estroff JA, Barnewolt CE, Connolly SA, Warfield SK. Fetal brain volumetry through MRI volumetric reconstruction and segmentation. Int J Comput Assist Radiol Surg. 2011;6(3):329–339. [PubMed: 20625848]
35. Gholipour A, Rollins CK, Velasco-Annis C, et al. A normative spatiotemporal MRI atlas of the fetal brain for automatic segmentation and analysis of early brain growth. Scientific Reports. 2017;7(1). doi:10.1038/s41598-017-00525-w
36. Gholipour A, Limperopoulos C, Clancy S, et al. Construction of a deformable spatiotemporal MRI atlas of the fetal brain: evaluation of similarity metrics and deformation models. Med Image Comput Comput Assist Interv. 2014;17(Pt 2):292–299. [PubMed: 25485391]
37. Gholipour A, Akhondi-Asl A, Estroff JA, Warfield SK. Multi-atlas multi-shape segmentation of fetal brain MRI for volumetric and morphometric analysis of ventriculomegaly. Neuroimage. 2012;60(3):1819–1831. [PubMed: 22500924]
38. Hoffmann M, Abaci Turk E, Gagoski B, et al. Rapid head-pose detection for automated slice prescription of fetal-brain MRI. Int J Imaging Syst Technol. 2021;(ima.22563). doi:10.1002/ima.22563
39. Moyer D, Turk EA, Ellen Grant P, Wells WM, Golland P. Equivariant Filters for Efficient Tracking in 3D Imaging. arXiv [csCV]. Published online March 18, 2021. http://arxiv.org/abs/2103.10255
40. Xu J, Lala S, Gagoski B, et al. Semi-supervised Learning for Fetal Brain MRI Quality Assessment with ROI Consistency. In: Medical Image Computing and Computer Assisted Intervention – MICCAI 2020. Springer International Publishing; 2020:386–395.

41. Gagoski B, Xu J, Wighton P, et al. Automatic detection and reacquisition of motion degraded images in fetal HASTE imaging at 3T. In: Proceedings of the ISMRM 28th Annual Meeting & Exhibition. ; 2020.
42. Mirsky DM, Shekdar KV, Bilaniuk LT. Fetal MRI: Head and Neck. Magn Reson Imaging Clin N Am. 2012;20(3):605–618. [PubMed: 22877957]
43. Feygin T, Khalek N, Moldenhauer JS. Fetal brain, head, and neck tumors: Prenatal imaging and management. Prenat Diagn. 2020;40(10):1203–1219. [PubMed: 32350893]
44. Gholipour A, Estroff J a., Warfield SK. Robust super-resolution volume reconstruction from slice acquisitions: application to fetal brain MRI. IEEE Trans Med Imaging. 2010;29(10):1739–1758. [PubMed: 20529730]
45. Kuklisova-Murgasova M, Quaghebeur G, Rutherford MA, Hajnal JV, Schnabel JA. Reconstruction of fetal brain MRI with intensity matching and complete outlier removal. Med Image Anal. 2012;16(8):1550–1564. [PubMed: 22939612]
46. Kim K, Habas P a., Rousseau F, Glenn O a., Barkovich AJ, Studholme C. Intersection based motion correction of multislice MRI for 3-D in utero fetal brain image formation. IEEE Trans Med Imaging. 2010;29(1):146–158. [PubMed: 19744911]
47. Uus A, Zhang T, Jackson LH, et al. Deformable Slice-to-Volume Registration for Motion Correction of Fetal Body and Placenta MRI. IEEE Trans Med Imaging. Published online February 18, 2020. doi:10.1109/TMI.2020.2974844
48. Kainz B, Steinberger M, Wein W, et al. Fast Volume Reconstruction from Motion Corrupted Stacks of 2D Slices. IEEE Trans Med Imaging. 2015;34(9):1901–1913. [PubMed: 25807565]
49. Lloyd DFA, Pushparajah K, Simpson JM, et al. Three-dimensional visualisation of the fetal heart using prenatal MRI with motion corrected slice-volume registration. Lancet. 2018;Accepted. (18):1–10.
50. Ebner M, Wang G, Li W, et al. An automated framework for localization, segmentation and super-resolution reconstruction of fetal brain MRI. Neuroimage. 2020;206:116324.
51. Arefeen Y, Arango N, Iyer S, et al. Refined-subspaces for two iteration single shot T2-Shuffling using dictionary matching. In: Proceedings of the ISMRM 27th Annual Meeting & Exhibition.
52. Arefeen Y, Gagoski B, Turk E, et al. Single-shot T2-weighted Fetal MRI with variable flip angles, full k-space sampling, and nonlinear inversion: towards improved SAR and sharpness. In: Proc. ISMRM Annual Meeting, Paris. ; 2020:2574.
53. Singh A, Salehi SSM, Gholipour A. Deep Predictive Motion Tracking in Magnetic Resonance Imaging: Application to Fetal Imaging. IEEE Trans Med Imaging. 2020;39(11):3523–3534. [PubMed: 32746102]
54. Hayat TTA, Nihat A, Martinez-Biarge M, et al. Optimization and initial experience of a multisection balanced steady-state free precession cine sequence for the assessment of fetal behavior in utero. AJNR Am J Neuroradiol. 2011;32(2):331–338. [PubMed: 21087938]
55. Nagaraj UD, Kline-Fath BM. Imaging of open spinal dysraphisms in the era of prenatal surgery. Pediatr Radiol. 2020;50(13):1988–1998. [PubMed: 33252764]
56. Adzick NS, Thom EA, Spong CY, et al. A randomized trial of prenatal versus postnatal repair of myelomeningocele. N Engl J Med. 2011;364(11):993–1004. [PubMed: 21306277]
57. Coleman BG, Langer JE, Horii SC. The diagnostic features of spina bifida: the role of ultrasound. Fetal Diagn Ther. 2015;37(3):179–196. [PubMed: 25341807]
58. Aaronson OS, Hernanz-Schulman M, Bruner JP, Reed GW, Tulipan NB. Myelomeningocele: Prenatal Evaluation—Comparison between Transabdominal US and MR Imaging. Radiology. 2003;227(3):839–843. [PubMed: 12714679]
59. Jackson LH, Price AN, Hutter J, et al. Respiration resolved imaging with continuous stablestate 2D acquisition using linear frequency SWEEP. Magn Reson Med. 2019;82(5):1631–1645. [PubMed: 31183892]
60. Jackson LH, Uus A, Batalle D, et al. Motion corrected reconstruction of abdominal SWEEP data using local similarity graphs and deformable slice to volume registration. In: Proc Intl Soc Mag Reson Med. ; 2020:453.
61. Afacan O, Estroff JA, Yang E, et al. Fetal Echoplanar Imaging: Promises and Challenges. Top Magn Reson Imaging. 2019;28(5):245–254. [PubMed: 31592991]

62. Lees CC, Stampalija T, Baschat A, et al. ISUOG Practice Guidelines: diagnosis and management of small-for-gestational-age fetus and fetal growth restriction. Ultrasound Obstet Gynecol. 2020;56(2):298–312. [PubMed: 32738107]
63. Poustchi-Amin M, Mirowitz SA, Brown JJ, McKinstry RC, Li T. Principles and applications of echo-planar imaging: a review for the general radiologist. Radiographics. 2001;21(3):767–779. [PubMed: 11353123]
64. Lustig M, Donoho D, Pauly JM. Sparse MRI: The application of compressed sensing for rapid MR imaging. Magn Reson Med. 2007;58(6):1182–1195. [PubMed: 17969013]
65. Feinberg DA, Hale JD, Watts JC, Kaufman L, Mark A. Halving MR imaging time by conjugation: demonstration at 3.5 kG. Radiology. 1986;161(2):527–531. [PubMed: 3763926]
66. Pruessmann KP, Weiger M, Scheidegger MB, Boesiger P. SENSE: Sensitivity encoding for fast MRI. Magn Reson Med. 1999;42(5):952–962. [PubMed: 10542355]
67. Griswold MA, Jakob PM, Heidemann RM, et al. Generalized autocalibrating partially parallel acquisitions (GRAPPA). Magn Reson Med. 2002;47(6):1202–1210. [PubMed: 12111967]
68. Wang F, Dong Z, Reese TG, et al. Echo planar time-resolved imaging (EPTI). Magn Reson Med. 2019;81(6):3599–3615. [PubMed: 30714198]
69. Feinberg DA, Setsompop K. Ultra-fast MRI of the human brain with simultaneous multi-slice imaging. J Magn Reson. 2013;229:90–100. [PubMed: 23473893]
70. Turk EA, Abulnaga SM, Luo J, et al. Placental MRI: Effect of maternal position and uterinecontractions on placental BOLD MRI measurements. Placenta. 2020;95(April):69–77. [PubMed: 32452404]
71. Xu J, Zhang M, Turk EA, Ellen Grant P, Golland P, Adalsteinsson E. 3D Fetal Pose Estimation with Adaptive Variance and Conditional Generative Adversarial Network. Medical Ultrasound, and Preterm, Perinatal and Paediatric Image Analysis. Published online 2020:201–210. doi:10.1007/978-3-030-60334-2_20
72. Zhang M, Xu J, Abaci Turk E, Grant PE, Golland P, Adalsteinsson E. Enhanced Detection of Fetal Pose in 3D MRI by Deep Reinforcement Learning with Physical Structure Priors on Anatomy. In: Medical Image Computing and Computer Assisted Intervention – MICCAI 2020. Springer International Publishing; 2020:396–405.
73. Sobotka D, Licandro R, Ebner M, et al. Reproducibility of Functional Connectivity Estimatesin Motion Corrected Fetal fMRI. Smart Ultrasound Imaging and Perinatal, Preterm and Paediatric Image Analysis. Published online 2019:123–132. doi:10.1007/978-3-030-32875-7_14
74. Turk E, van den Heuvel MI, Benders MJ, et al. Functional Connectome of the Fetal Brain. J Neurosci. 2019;39(49):9716–9724. [PubMed: 31685648]
75. Figueiredo CM, Falcão I, Vilaverde J, et al. Prenatal Diagnosis and Management of a Fetal Goiter Hypothyroidism due to Dyshormonogenesis. Case Rep Endocrinol. 2018;2018:9564737. [PubMed: 30662777]
76. Machado CM, Castro JM, Campos RA, Oliveira MJ. Graves' disease complicated by fetal goitrous hypothyroidism treated with intra-amniotic administration of levothyroxine. BMJ Case Rep. 2019;12(8). doi:10.1136/bcr-2019-230457
77. Li T-G, Zhang Y-Y, Nie F, Peng M-J, Li Y-Z, Li P-L. Diagnosis of foetal vein of galen aneurysmal malformation by ultrasound combined with magnetic resonance imaging: a case series. BMC Med Imaging. 2020;20(1):63. [PubMed: 32532203]
78. Block KT, Chandarana H, Fatterpekar G, et al. Improving the robustness of clinical T1-weighted MRI using radial VIBE. Magnetom Flash. 2013;5:6–11.
79. Morgan L. Development of a 3D radial MR Imaging sequence to be used for (self) navigation during the scanning of the fetal brain in utero. Published online 2016. https://open.uct.ac.za/handle/11427/22735
80. Haskell MW, Cauley SF, Wald LL. TArgeted Motion Estimation and Reduction (TAMER): Data Consistency Based Motion Mitigation for MRI Using a Reduced Model Joint Optimization. IEEE Transactions on Medical Imaging. 2018;37(5):1253–1265. doi:10.1109/tmi.2018.2791482 [PubMed: 29727288]

81. Haskell MW, Cauley SF, Bilgic B, et al. Network Accelerated Motion Estimation and Reduction (NAMER): Convolutional neural network guided retrospective motion correction using a separable motion model. Magn Reson Med. 2019;82(4):1452–1461. [PubMed: 31045278]
82. Stirnemann J, Chalouhi G, Essaoui M, et al. Fetal brain imaging following laser surgery in twin-to-twin surgery. BJOG. 2018;125(9):1186–1191. [PubMed: 27348600]
83. Prsa M, Sun L, van Amerom J, et al. Reference Ranges of Blood Flow in the Major Vessels of the Normal Human Fetal Circulation at Term by Phase Contrast Magnetic Resonance Imaging. Circ Cardiovasc Imaging. Published online May 29, 2014. doi:10.1161/CIRCIMAGING.113.001859
84. Salehi D, Sun L, Steding-Ehrenborg K, et al. Quantification of blood flow in the fetus with cardiovascular magnetic resonance imaging using Doppler ultrasound gating: Validation against metric optimized gating. J Cardiovasc Magn Reson. 2019;21(1):1–15. [PubMed: 30612574]
85. Zhu MY, Milligan N, Keating S, et al. The hemodynamics of late onset intrauterine growth restriction by MRI. Am J Obstet Gynecol. 2015;7:195–225.
86. Grevent D, Taso M, Millischer A, et al. OC07.07: SS□FSE FAIR ASL parameters for non□invasive measurement of fetal brain perfusion in vivo. Ultrasound Obstet Gynecol. 2019;54(S1):18–18.
87. Francis ST, Duncan KR, Moore RJ, Baker PN, Johnson IR, Gowland PA. Non-invasive mapping of placental perfusion. Lancet. 1998;351(9113):1397–1399. [PubMed: 9593410]
88. Harteveld AA, Hutter J, Franklin SL, et al. Systematic evaluation of velocity-selective arterial spin labeling settings for placental perfusion measurement. Magn Reson Med. 2020;84(4):1828–1843. [PubMed: 32141655]
89. Zun Z, Zaharchuk G, Andescavage NN, Donofrio MT, Limperopoulos C. Non-Invasive Placental Perfusion Imaging in Pregnancies Complicated by Fetal Heart Disease Using Velocity-Selective Arterial Spin Labeled MRI. Sci Rep. 2017;(November):1–10. [PubMed: 28127051]
90. Sun L, Macgowan CK, Sled JG, et al. Reduced fetal cerebral oxygen consumption is associated with smaller brain size in fetuses with congenital heart disease. Circulation. 2015;131(15):1313–1323. [PubMed: 25762062]
91. Rodríguez-Soto AE, Langham MC, Abdulmalik O, Englund EK, Schwartz N, Wehrli FW. MRI quantification of human fetal O2delivery rate in the second and third trimesters of pregnancy. Magn Reson Med. 2018;80(3):1148–1157. [PubMed: 29359353]
92. Turk EA, Stout JN, Ha C, et al. Placental MRI: Developing Accurate Quantitative Measures of Oxygenation. Top Magn Reson Imaging. 2019;(Special Issue on Placental Imaging). https://docs.google.com/document/d/1E9LWkCdzYrHpN-cVLupP8IPxp9zFFGAiM6LMZBiKiRk/edit
93. Freud LR, Tworetzky W. Fetal interventions for congenital heart disease. Current Opinion in Pediatrics. 2016;28(2):156–162. doi:10.1097/mop.0000000000000331 [PubMed: 26886784]
94. Orbach D. Fetal treatment for vein of Galen malformations. Published June 12, 2019. Accessed February 19, 2021. https://discoveries.childrenshospital.org/fetal-treatment-vein-of-galen-malformations/

Synopsis

MRI is used in conjunction with ultrasound screening for fetal brain abnormalities since it offers better contrast, higher resolution, and has multiplanar capabilities that increase the accuracy and confidence of diagnosis. Fetal motion still severely limits the MRI sequences that can be acquired. We outline the current acquisition strategies for fetal brain MRI, and discuss the near term advances that will improve its reliability. Prospective and retrospective motion correction aim to make the complement of MR neuroimaging modalities available for fetal diagnosis, improve the performance of existing modalities, and open new horizons to understanding in utero brain development.

Key points:

1. US and MRI are complementary, and will likely remain so,even with future MRI advances. MR provides crucial additional information regarding brain structure
2. MR imaging of the developing brain, face/neck and spine of the fetus is complex, but crucial for optimal fetal management when there are suspected abnormalities. Interpreting and reporting fetal MRI requires not only a deep understanding of embryology, normal development and common malformations, but also a clear sense of the MR sequences currently available for clinical use, their strengths and limitations as well as common artifacts.
3. Significant improvements in clinical MRI protocols are within reach.
4. Physiology and function are long term goals of ongoing MRI sequence development and post acquisition analysis techniques.

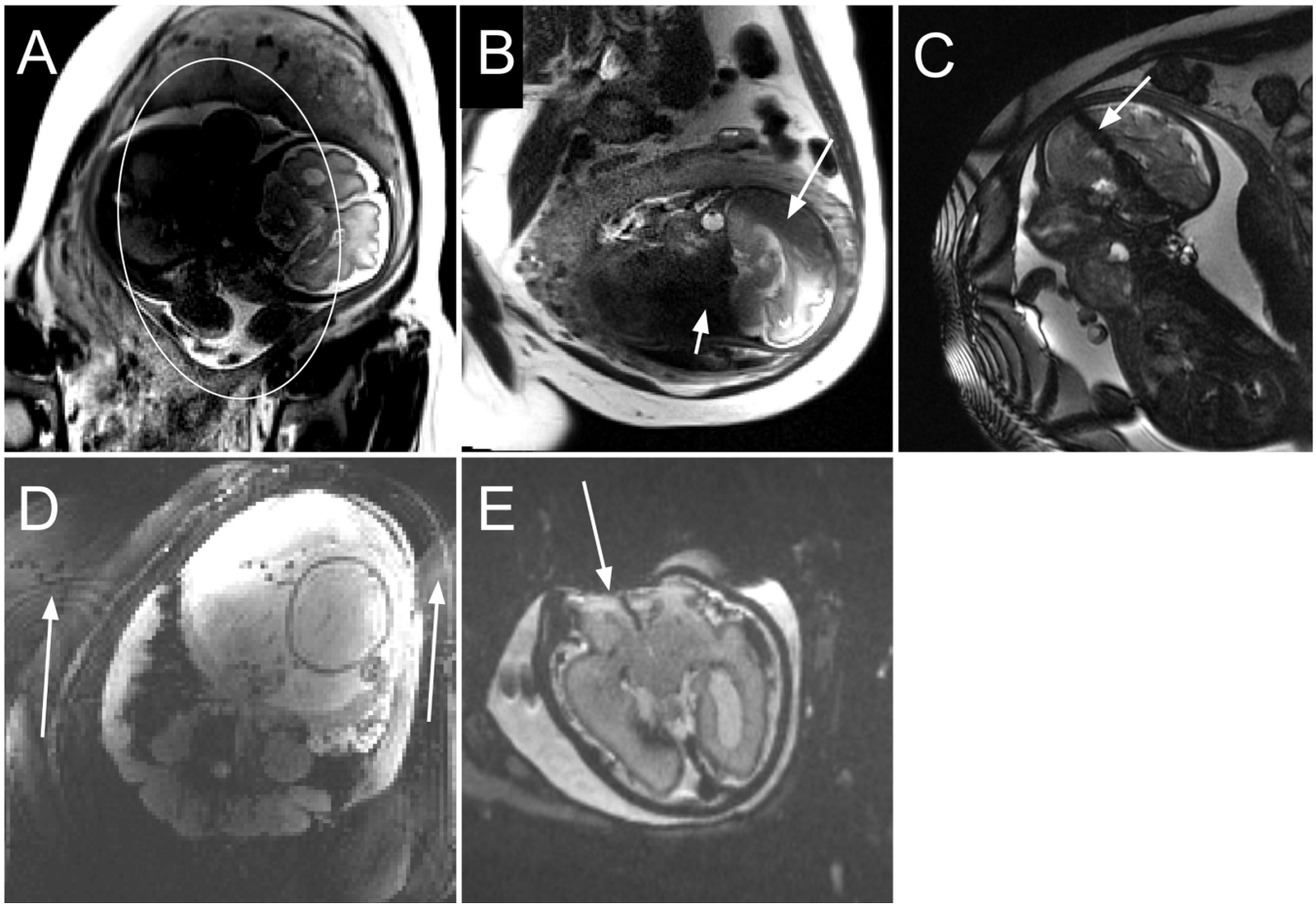

Figure 1.

Common artifacts of fetal MRI. **(A)** The dielectric artifact (low signal intensity in the central part of the image, circle) is caused by the size of the abdomen in comparison to the frequency of the RF pulses used in imaging. **(B)** SS-FSE slice corruption (low signal intensity in the anterior and inferior areas of the head, arrows) due to fetal motion, and volume incoherence also causes information loss. **(C)** bSSFP banding (one dark band crosses the brain, arrow) is caused by magnetic field inhomogeneities. EPI artefacts include **(D)** ghosting (image copies, arrows), **(E)** geometric distortion (anterior aspect of brain is distorted, arrow) likely caused by proximity to the maternal bowel, and susceptibility artefact as shown in Figure 9.

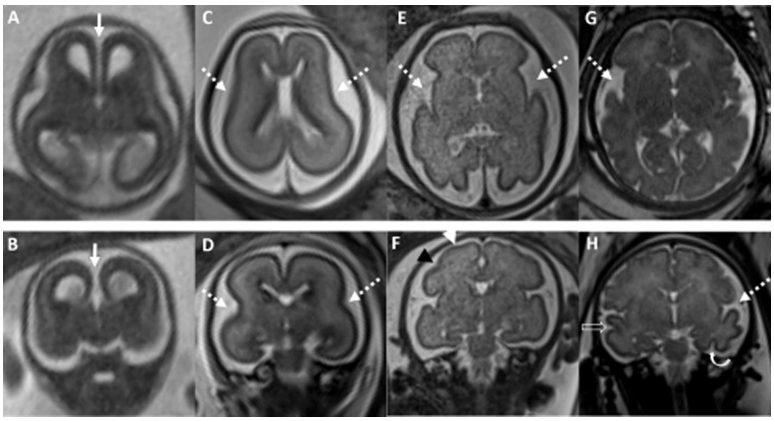

Figure 2.

Normal progresive development of cerebral sulcation in the fetal brain at different gestational ages. Axial and coronal SS-FSE images in 4 different fetuses. **(A,B)** 15 weeks, 6 days of gestational age; **(C,D)** 22 weeks, 2 days of gestational age; **(E,F)** 28 weeks, 3 days of gestational age and **(G,H)** 34 weeks, 0 days gestational age. Interhemispheric fissure (*arrow*) sylvian fissures *(dashed arrows),* superior frontal sulcus *(white arrowhead),* inferior frontal sulcus *(black arrowhead),* inferior temporal sulcus *(curved arrow)* and superior temporal sulcus *(open arrow).*

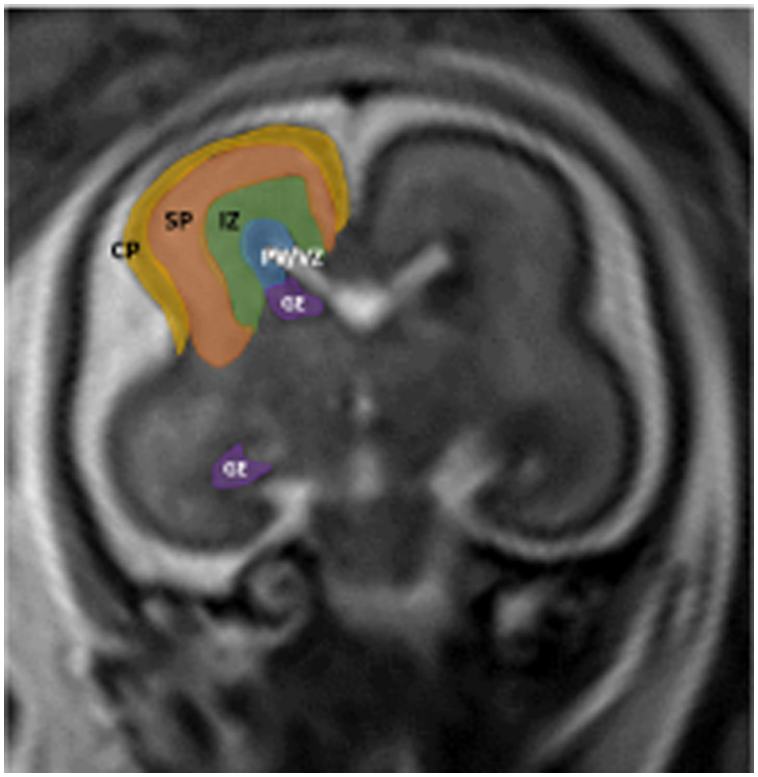

Figure 3.
Normal multilaminar appearance of the brain parenchyma in a fetus with 22 weeks of gestation. Coronal SS-FSE image. VZ= ventricular zone, PV= periventricular fiber-rich zone, IZ= intermediate zone, SP= subplate, CP= cortical plate and GE= ganglionic eminences.

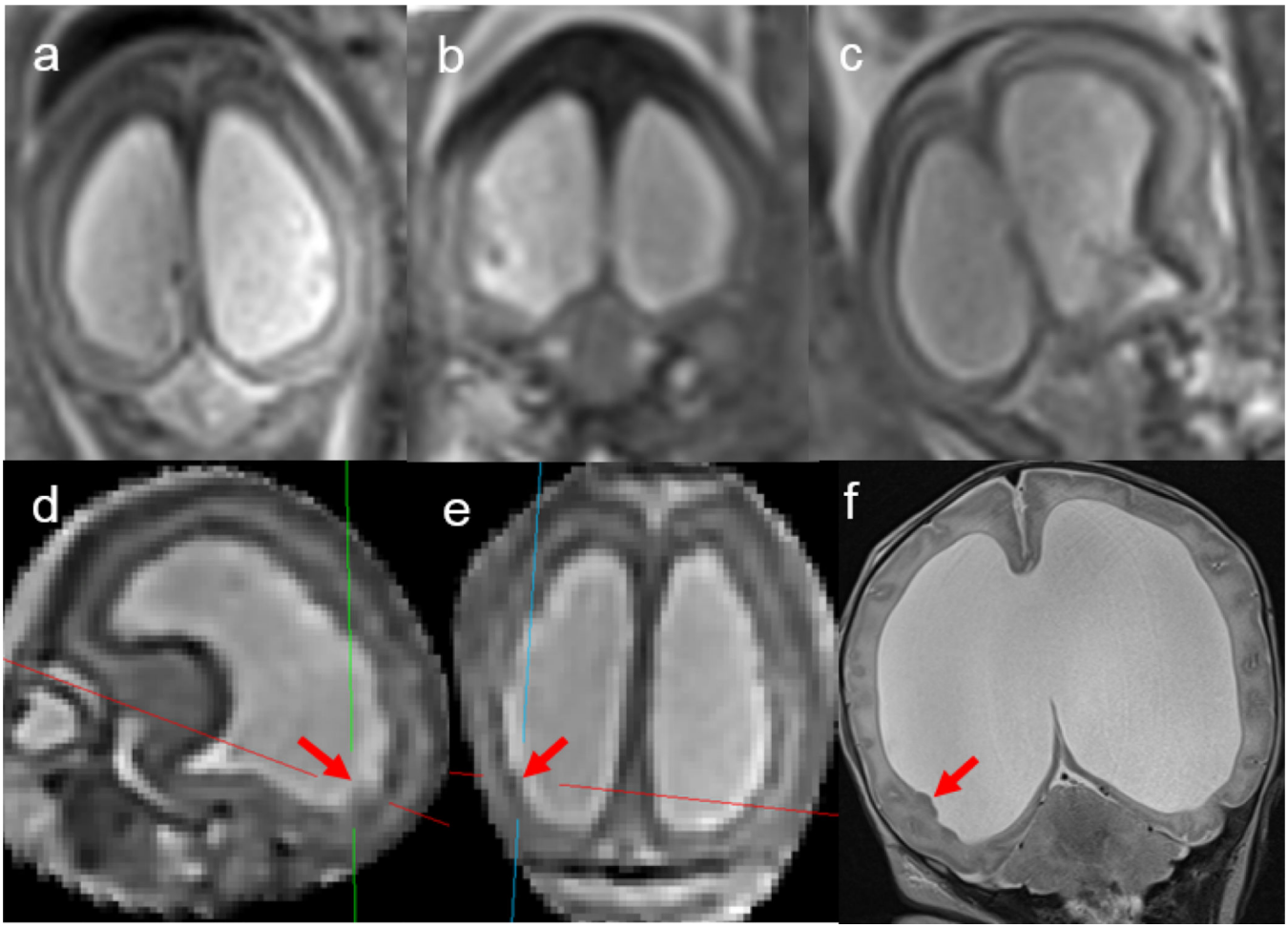

Figure 4.

Coherent fetal volumes improve identification of subependymal gray matter heterotopia in a fetus with 22 weeks of gestation. **(A, B, C)** Coronal images from 3 different SS-FSE stacks. No heterotopias were prospectively identified by two experienced fetal neuroradiologists. **(D, E)** SVR reconstruction enables the detection of a focus of subependymal heterotopia (red arrows) due to the ability to cross-reference it in a coherent volume. **(F)** Postnatal T2-weighted image confirmed the focus of heterotopia (red arrow). Coherent fetal volumes have the potential to improve diagnostic accuracy.

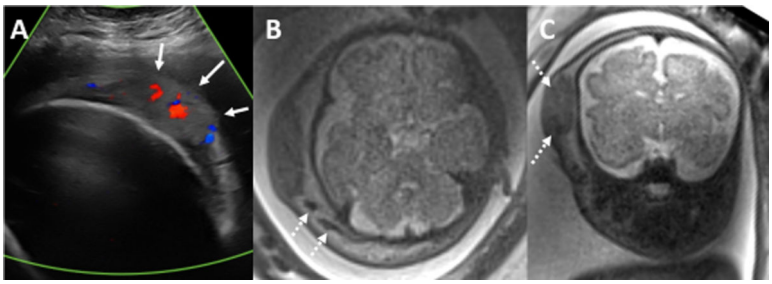

Figure 5.

Scalp congenital hemangioma in a fetus at 32 weeks of gestation. **(A)** Transverse color doppler image of the right scalp demonstrates a well circumscribed hypoechoic subcutaneous mass with increased vascularity of color doppler interrogation *(arrows).* The mass demonstrated venous and arterial waveforms (not shown). **(B)** Axial and **(C)** coronal SS-FSE images show diffuse right-sided scalp swelling surrounding the soft tissue mass. There are multiple foci of linear low signal around and within the mass *(dashed arrows)* consistent with flow voids. There is remodeling of the skull without intracranial extension.

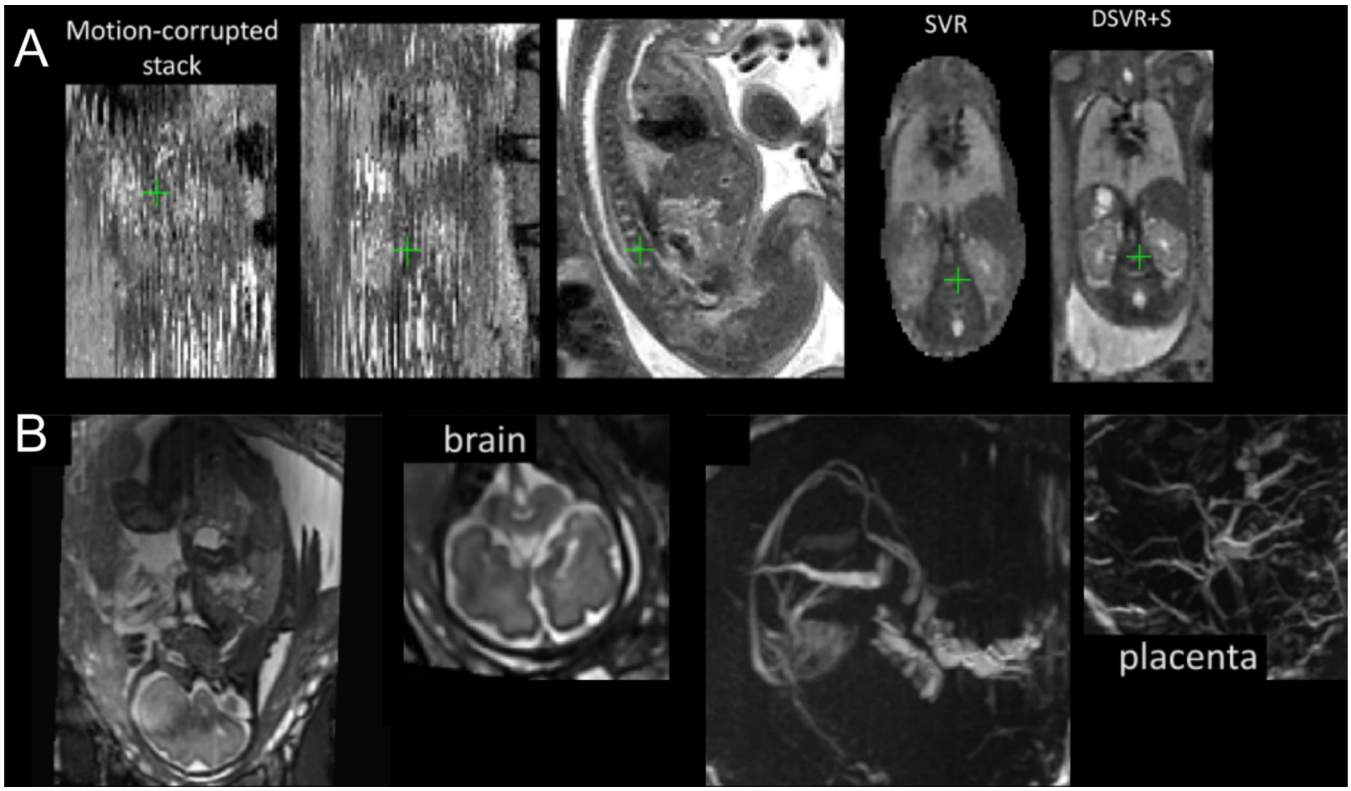

Figure 6.

Examples of 3D volume reconstructions. **(A)** A recently proposed 3D reconstruction algorithm relaxes the rigid body constraints of prior slice-to-volume registration (SVR) techniques. Here a deformable slice to volume registration, super resolution reconstruction with integrated outlier removal (DSVR+S) recovers a high quality isotropic volume from the heavily motion corrupted acquisition on the left. (Adapted from Uus A, et al. Deformable Slice-to-Volume Registration for Motion Correction of Fetal Body and Placenta MRI. IEEE Trans Med Imaging. Published online February 18, 2020; with permission) **(B)** DSVR can be combined with novel acquisition strategies, here an excitation scheme that produces an imaging volume by continuously moving an excitation band across the volume of interest (SWEEP), to produce high quality structural (left) and angiographic (right) volumes. (From Jackson LH, et al. Motion corrected reconstruction of abdominal SWEEP data using local similarity graphs and deformable slice to volume registration. In: Proc Intl Soc Mag Reson Med.; 2020:453.; with permission)

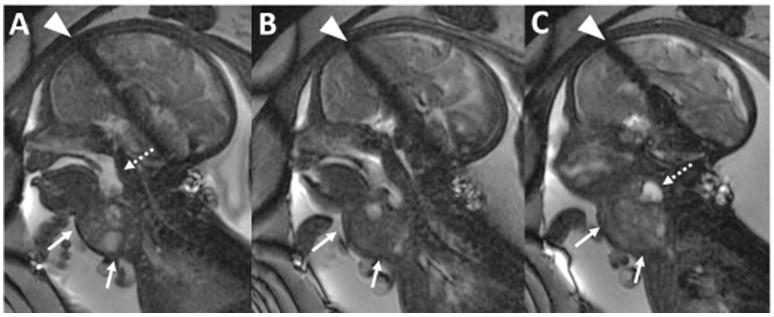

Figure 7.

Airway narrowing and swallowing impairment in a fetus with 34 weeks of gestation due to mass effect from cervical teratoma. **(A-C)** Sagittal bSSFP cine clips show a predominantly solid mass in the anterior cervical region with macrocystic changes consistent with postnatally confirmed cervical teratoma *(arrows)*. Dynamic assessment of the airways and esophagus demonstrate dilation of the hypopharynx *(dashed arrows)* and no clear visualization of the upper esophageal distention consistent with mass effect in the airway. This fetus also presented with polyhydramnios (not shown). Note the banding artifact *(arrowhead)* related to this sequence.

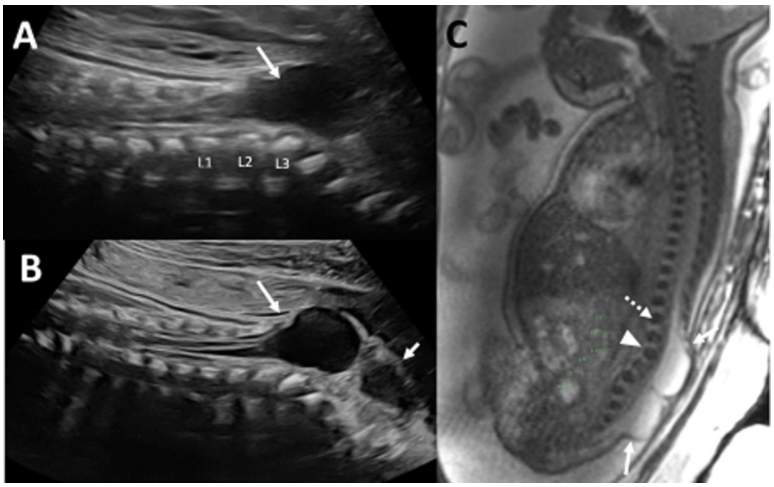

Figure 8.

Complex open neural defect in a fetus with 35 weeks of gestation. **(A, B)** Sagittal ultrasound images of the lumbosacral region shows a complex bilobed myelomeningocele *(arrows).* The exact level of spinal defect is difficult to identify on ultrasound due to kyphosis centered at L3. **(C)** Sagittal bSSFP demonstrates spinal defect extending from about L1 *(dashed arrow)* through the sacrum *(arrows).* There is a lumbosacral kyphotic curve centered at L3 *(arrow head).* In addition, MRI showed moderate ventriculomegaly and mild inferior displacement of the cerebellar tonsils (Not shown) consistent with Chiari II malformation.

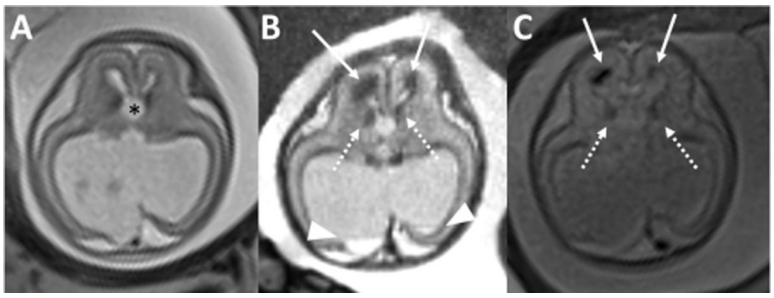

Figure 9.

Intraventricular bleeding as cause of ventriculomegaly in a fetus with 20 weeks of gestation **(A)** Axial SS-FSE image demonstrates severe lateral ventriculomegaly and moderate dilation of the third ventricle *(*).* The fourth ventricle was normal in size (not shown). **(B)** EPI T2* image with high TE (80ms) demonstrate fluid-fluid level in the lateral ventricles *(arrowheads)* and foci of susceptibility artifacts in the bilateral frontal periventricular white matter *(arrows)* and the bilateral caudothalamic grooves *(dashed-arrows)* consistent with germinal matrix hemorrhage with parenchymal and intraventricular extension, and the likely cause of the ventriculomegaly. Note geometric distortion artifact of in the anterior cranium and frontal lobes. **(C)** EPI T2* image with low TE (30ms) confirmed presence of susceptibility artifacts seen on the high TE sequence.

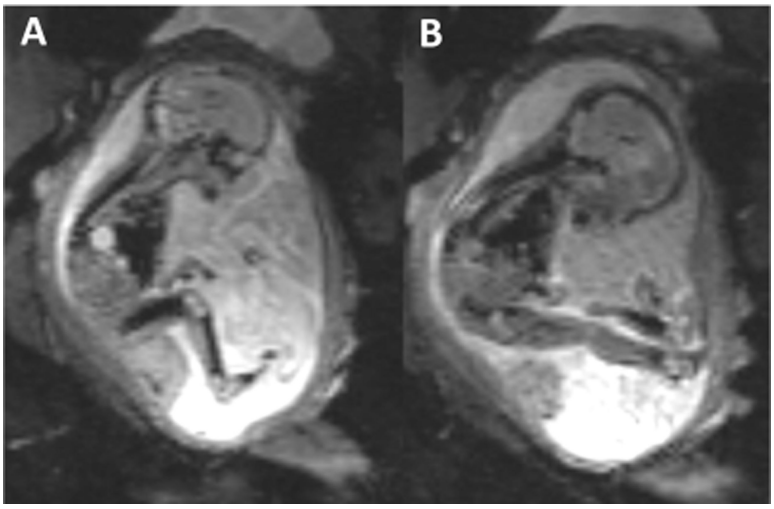

Figure 10.

Normal subjective fetal motion of the right lower extremity in a fetus with 19 weeks of gestation. **(A, B)** Sagittal GRE-EPI sequence acquired as a cine clip demonstrates flexion and extension of the left knee and ankle. Note that the cartilaginous epiphyses appear as high signal and the cortical bone of the diaphyses are low signal.

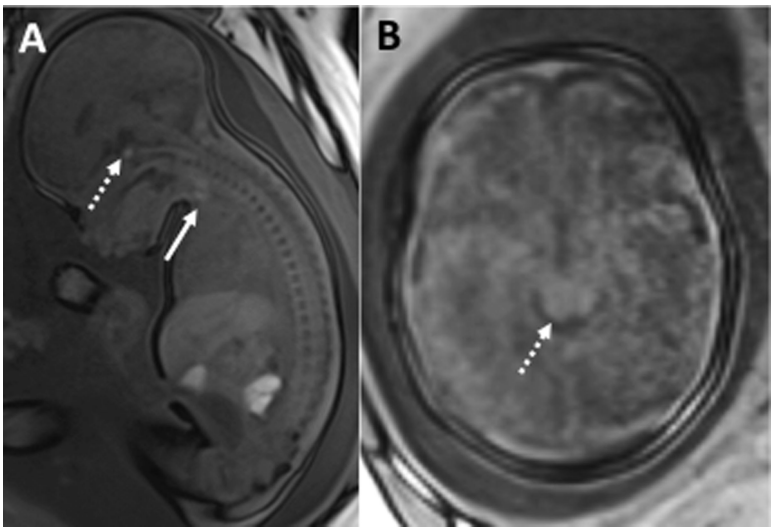

Figure 11.

Normal T1-weighted images in a fetus of 34 week of gestation **(A)** Sagittal T1-weighted image shows the normal T1 hyperintense thyroid pituitary gland *(dashed arrow*) and thyroid gland *(arrow).* **(B)** Axial T1-weighted images in the same fetus show normal myelination with T1 shortening in the tegmentum of the pons (*dashed arrow*). Note the T1-contrast and lower SNR compared to SS-FSE sequence in fetus Figure 2 (G, H).

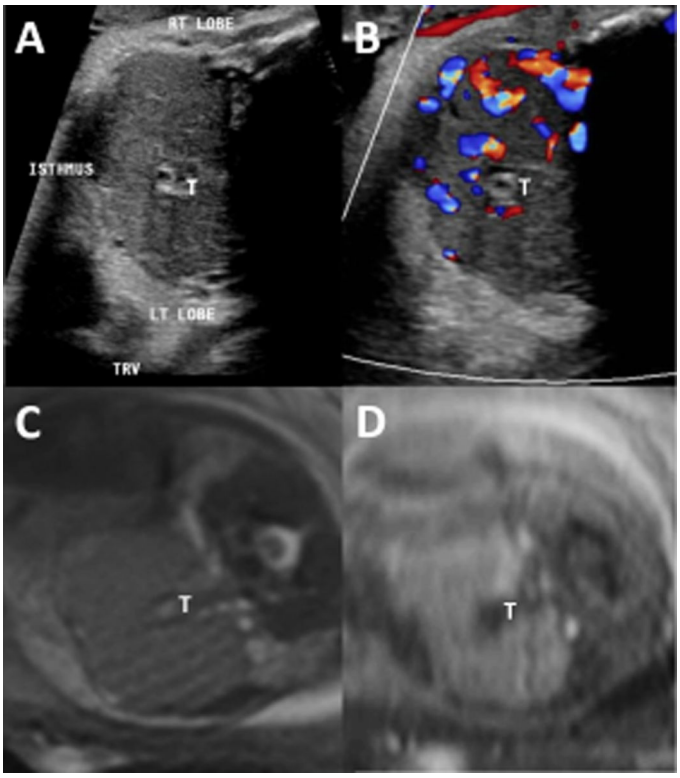

Figure 12.

Fetal Goiter in a fetus with 33 weeks of gestational age. **(A)**Transverse grayscale and **(B)** color doppler sonographic image of the neck demonstrates a solid, bilobed homogeneous midline mass around the traquea (T) with increased vascularity in color doppler interrogation. **(C)** Axial balanced SSFP and **(D)** axial T1-weighted images of the neck show that this bilobed mass demostraste high signal of T1-weighted images consistent with thyroid tissue.

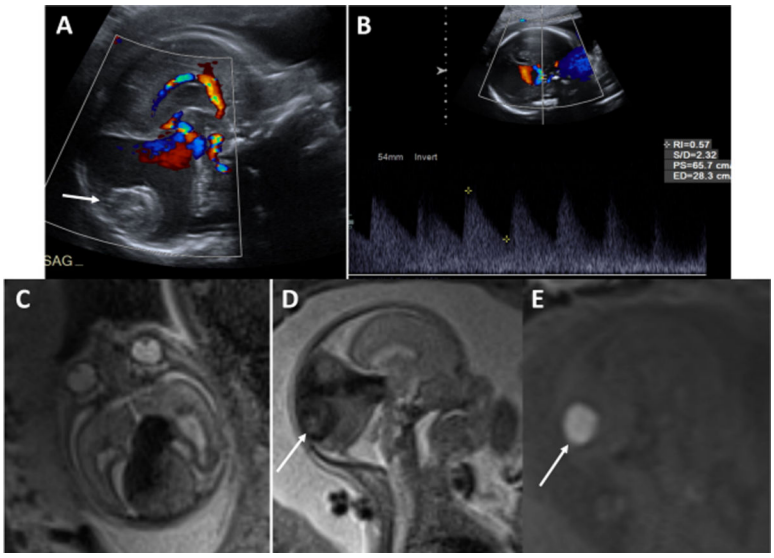

Figure 13.

Partially thrombosed dural sinus malformation in a fetus with 21 weeks of gestation. **(A)** Doppler ultrasound image in the sagittal plane shows a large midline predominantly anechoic structure at the torcula level with prominent flow in the anterior aspect, consistent with a large dural sinus malformation. There is an isoechoic round focus in the posterior margin without vascular flow *(arrow)*. **(B)** Spectral doppler image in the sagittal plane demonstrates arterial flow along the anterior margin of the malformation, suggesting presence of arteriovenous communication. **(C)** Axial and **(D)** sagittal SS-FSE images demonstrate a large dural sinus malformation with predominant T2 hypointense signal. **(E)** T1-weighted sagittal image at the same level as (D) demonstrates a round high signal focus *(arrow)* consistent with an intralesional thrombus.

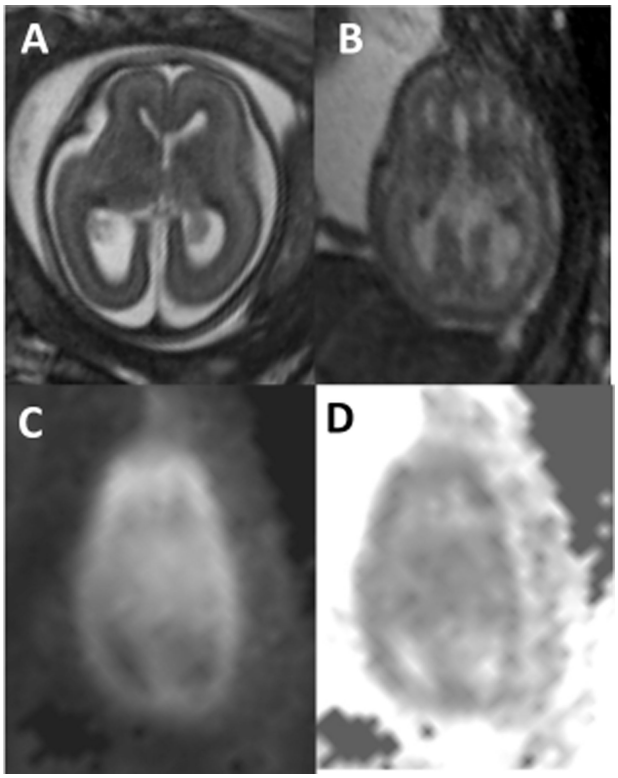

Figure 14.

Fetal demise of fetus B, status post 8 days of laser ablation therapy for twin-twin transfusion syndrome in a 22 weeks gestation. **(A)** Axial bSSFP images of fetus A shows mild right ventriculomegaly with normal appearance of the extra-axial fluid spaces for gestational age. **(B)** Axial bSSFP images of fetus B shows nonspecific diffuse decrease in extra-axial fluid spaces with normal ventricular size. The calvarium of fetus B is smaller compared to fetus A. **(C)** Axial B-500 image and **(D)** ADC maps demonstrate global brain parenchymal diffusion restriction consistent with fetal demise.

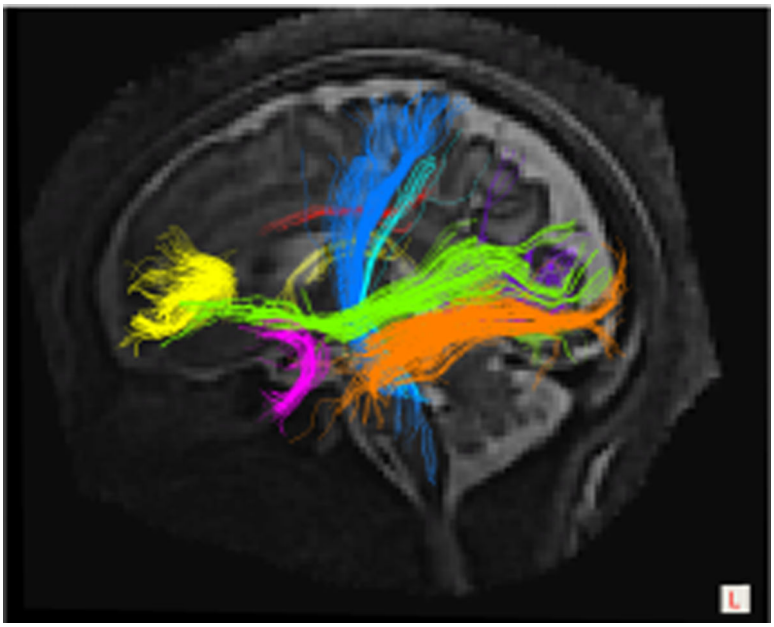

Figure 15.

Reconstructed diffusion tensor images (DTI) in a fetus with 36 weeks of gestation shows white matter fiber bundles of the brain (images courtesy of Camilo Jaimes Cobos, MD, and Fedel Machado, MD).

Table 1.

Applications, advantages and disadvantages of various fetal imaging modalities.

Modality or sequence	Applications	Advantages	Disadvantages
Ultrasound	• Screening for fetal brain and body abnormalities • Follow up of characterized fetal abnormalities • Fetal biometry • Doppler assessment of the fetus and placenta: • calculation of cerebroplacental index • Fetal echocardiogram	• Non-ionizing radiation. • Lower cost and higher availability • High spatial resolution. Good for assessment of the face (lips, nose, orbits) • High temporal resolution. Good for evaluation of fetal movement • Extensive normative biometric data • More reliable evaluation of cranial size • Doppler assessment of the fetal intracranial vasculature (Fetal Middle cerebral artery) and placenta • 3D evaluation of the face	• Operator dependant • Limited beam penetration and fetal assessment in cases of oligo- and anhydramnios, anterior placenta and maternal obesity • Lower sensitivity in characterization of fetal central nervous system abnormalities compared to MRI • Lower penetration of the skull with increasing gestational age due to ossification of the skull
SS-FSE	• Overall fetal body and brain anatomy • Anatomical detail ○ Brain ○ Face ○ Lips ○ Spinal cord • Reconstruction for high resolution brain volumes	• Single-shot (fast acquisition, freezing fetal motion) • Volume reconstruction is possible • High-resolution anatomical imaging	• Incoherent volume • Contrast (blurred approximation of T2 contrast) • Resolution/FOV tradeoff • High SAR
bSSFP	• Overall anatomy • Bright-blood sequence for evaluation of heart and vessels • Dynamic evaluation with cine clips (Extremity, fetal movement and swallowing)	• High SNR • Cine acquisition	• Poor tissue contrast • Requires very good magnetic field homogeneity to prevent banding artifacts
GRE EPI	• Identification of intracranial blood products • Assessing the bony components of the fetal spine	• Susceptibility artifacts aim in the identification of intracranial blood products • Good cortical bone assessment	• Extensive susceptibility artifacts • Image distortion • Low contrast resolution
T1w 3D GRE	• Mostly fetal body indications (identification of meconium, liver, thyroid) • Fetal brain indications include identification of intracranial hemorrhage, tubers in tuberous sclerosis complex and myelination • Identification of thrombosed dural venous fistulas or vein of Galen Malformation	• Evaluation of structures that have intrinsic T1-shortening	• Prone to motion artifacts
DWI/DTI	• Identification of cerebral ischemia (fetal stroke and hypoxic-ischemic injury) • Identification of intracranial hemorrhage, cysts and fetal tumors • DTI: potential to reveal reveal neuro-connectivity and microstructural development	• Only available sequence to identify altered diffusion	• Prone to motion and susceptibility artifacts

bSSFP = Balanced steady-state free precession

DWI = Diffusion weighted imaging

DTI = Diffusion tensor imaging

EPI = Echoplanar imaging

FOV = Field of view

GRE = Gradient echo

SAR = specific absorption rate

SNR = Signal to noise ratio

SS-FSE= Single-shot fast spin echo

Table 2.

Example protocol from our institution conducted on Siemens 3T scanners (Skyra and Vida, Siemens, Healthineers, Erlangen, Germany). Scans are usually conducted using the Siemens 30-channel flexible body array combined with the 18-channel spine array. Total acquisition time (TA), field of view (FOV), repetition time (TR), echo time (TE).

Sequence	TA (m:s)	FOV (cm)	TR (ms)	TE (ms)	Flip angle (degrees)	voxel size (mm^3)	# of slices	Acceleration	Other Details
SS-FSE	1:24	30×30	1400	103	160	1.2×1.2×2.5	60	R_{GRAPPA} = 2	partial fourier=5/8; interleaved slice acquisition
bSSFP	0:36	32×32	4.16	1.77	75	1×1×2.5	40	R_{GRAPPA} = 2	
GRE-EPI (motion)	2:07	30×30	5500	37	90	2×2×2	70	R_{GRAPPA} = 2	Measurements=20; EPI factor=150; Echo spacing=0.65 ms; interleaved slice acquisition; partial fourier=7/8
GRE-EPI (high res)	0:09	25×25	8520	80	90	1×1×2	30	R_{GRAPPA} = 2	Measurements=1; EPI factor=250; Echo spacing=1.0 ms; interleaved slice acquisition; partial fourier=6/8
Multi-echo SMS EPI (motion, T2* quantification)	10:00	35×25	8100	18/47 / 76	90	3.2×3.2×3.2	70	R_{GRAPPA} = 2, SMS = 2	Measurements = 72; EPI factor = 110; Echo spacing=0.5 ms
T1-VIBE	0:9.2	30×30	3.64	1.35	9	1×1×2	40	R_{GRAPPA} = 2	Slab thickness=8 cm; No fat saturation; RF spoiling; 7/8 phase partial fourier, 6/8 slice partial fourier; no volume interpolation in the slice direction
DWI/DTI	1:01	30×30	3800	57	90	2×2×4	30	R_{GRAPPA} = 2	12 directions, b=0, 700 s/mm^2; interleaved slice acquisition; 6/8 partial fourier